

UNIVERSITY OF ABERDEEN

Department of Geography & Environment

MASTER IN GEOGRAPHIC INFORMATION SYSTEMS

DISSERTATION

VINEYARD MAPPING USING UAV ACQUIRED IMAGES

LUCA ZANCHETTA

Master's degree in Agricultural Science



Submitted in partial fulfilment of the requirements for the degree of M.Sc. in Geographical Information Systems (GIS) at the University of Aberdeen 1st August 2016

DECLARATION

This dissertation has been composed by me. It has not been accepted in any previous application for a degree, and the work of which it is a record has been done by me. All quotations have been distinguished by quotation marks and sources of information have been acknowledged in the text and cited in the list of references.

Signed _____  _____

Date 01/08/2016

Word count 14303

ACKNOWLEDGEMENT

I would like first of all to express my sincere appreciation for the help given me by Dr. David Green as a supervisor for this dissertation.

My special thanks are also for Mr. Massimo Zambon, owner of the farm in Valdobbiadene (Italy) where images were collected: he has the merit to produce the best wine of the world and his help in choosing the site for this project was fundamental for me.

ABSTRACT

In the recent years Unmanned Aerial Vehicles have become a steadily popular remote sensing tool and their use is expected to grow rapidly in many applications, for instance in Precision Agriculture. Even though Precision Agriculture is largely used since many years in broad acre farms, only recently studies have proved its beneficial impact on small farms as well, in particular in the viticultural sector, characterised by a high-value final product.

In this study two low-cost UAVs, in conjunction with two types of cameras have been employed to acquire images of a small vineyard at different bandwidths. In particular, the study focused in analysing quantitatively and qualitatively the intra-vineyard variability in a bid to provide to the farmer information to differentiate the agricultural practices management. The research had positive outcomes in recreating the plants canopy in three dimensions: normally this operation requires the use of Lidar sensors whose cost represents a barrier for small farms. Using photogrammetry software like Agisoft Photoscan was possible to create a dense points cloud similar to the one produced by Lidar at a considerably lower cost. Nevertheless, the quality of the images acquired with the camera provided with Red-Infrared bands sensor was poor and was not possible to create a four band Orthoimage necessary to process the Normalised Difference Vegetation Index, important to measure the vines vigour. From the dense cloud was possible to produce a very high resolution Digital Surface Model and Orthoimage.

The Digital Differential Model (representing the vineyard canopy) and the Digital Terrain Model, along with some derivatives as Slope, Aspect and Topographic Wetness Index were computed. The Red-Green-Blue Orthoimage of the vineyard were segmented and classified with eCognition whereby the 'non-vine' pixels were removed and the vineyard canopy separated from the rest of the image using a simplified Object Based Image Analysis algorithm.

Three variables calculated in the study (DTM, slope and TWI) were screened performing a cluster analysis to evaluate the presence of variability in the plot studied. In this specific case, results show that the size of the plot was probably too small to point out statistically significant difference to allow a differential management of the plants.

Keywords: UAV, precision viticulture, NIR/RGB, structure from motion, cluster analysis.

CONTENTS

CHAPTER 1 – INTRODUCTION

1.1 An insight of the global wine industry.....	8
1.2 The micro-climate of “Prosecco di Conegliano e Valdobbiadene DOCG	8
1.3 Introduction to Precision Viticulture (PV).....	10
1.4 Aim of the study.....	11

CHAPTER 2 – LITERATURE REVIEW

2.1 Introduction.....	13
2.2 Spatial variability in the vineyard.....	14
2.3 Overview of Unmanned aerial vehicles (UAV) image acquisition in PV.....	15
2.4 Vegetation Indexes.....	15
2.4.1 Leaf Area Index (LAI).....	16
2.4.2 Normalized Difference Vegetation Index (NDVI) and Plant Cell Density (PCD)...	16
2.5 Vineyard canopy reconstruction through Structure from motion.....	17
2.6 Object Based Image Analysis (OBIA).....	20
2.7 Vineyard zonation.....	21

CHAPTER 3 – METHODOLOGY

3.1 Important premise.....	23
3.2 Description of the area studied.....	24
3.3 Description of the UAVs, gimbals and cameras used to collect the data.....	27
3.3.1 <i>DJI Phantom 2 with Zenmuse H3-3D Gimbal and GoPro Hero 3+ silver edition..</i>	27
3.3.2 <i>3D Robotics IRIS+ with Tatot 2D Gimbal and Mapir Survey 2 NDVI camera.....</i>	30
3.3.3 <i>Description of the software and hardware used in this research.....</i>	33
3. 4 Data acquisition.....	34
3.4.1 <i>Ground Control Points (GCPs) placement and methodology propose in measuring the coordinates.....</i>	34
3.4.2 <i>Images collection.....</i>	36
3.5 Image pre-processing.....	38
3.5.1 <i>Introduction.....</i>	38
3.5.2 <i>Geocoding the images.....</i>	38
3.5.3 <i>Selecting the best images.....</i>	38
3.6 Image processing.....	39
3.6.1 <i>Building the 3D model of vineyard using Structure from Motion (SfM).....</i>	39
3.6.2 <i>RGB Image processing with Agisoft Photoscan.....</i>	40
3.6.3 <i>Red-Nir Image processing with Agisoft Photoscan.....</i>	42
3.6.4 <i>Red-NIR Image processing with Pix4DMapper.....</i>	43

3.6.5 Creation of Digital Difference Model (DDM).....	43
3.6.6 Derivatives of Digital Terrain Model (DTM) and preparation for cluster analysis.....	44
3.6.7 Vineyard canopy separation with eCognition.....	46
3.7 Cluster analysis	47

CHAPTER 4 – RESULTS

4.1 Introduction.....	49
4.2 Image processing results.....	49
4.3 Cluster analysis results.....	52

CHAPTER 5 – DISCUSSIONS

5.1 Introduction.....	75
5.2 Comment over the UAVS and cameras used.....	75
5.3 Canopy reconstruction.....	76
5.4 Cluster analysis.....	77

CHAPTER 5 – CONCLUSIONS.....78

CITED REFERENCES.....80

APPENDICE – CLIMATIC DATA.....87

CHAPTER 1 – INTRODUCTION

1.1 An insight of the global wine industry

The wine industry represents an important source of income for the economy of many Countries and in 2015 the world wine production was estimated to be 275.7 million hectolitres, showing a rise of 2% compare with the previous year. Italy, France and Spain are the world's largest producers. The viticultural sector itself, is very strategical as it contributes massively to the economy of those Countries as well as creates job opportunities. Although traditional countries have seen a fall in their cultivated hectares, this has been partially compensated by an increment in emerging Countries, some of them becoming large consumers and importers (i.e. China). (Source Morgan Stanley, 2013)

One of the most important aspects to be considered in the viticultural sector is the constant demand for high quality wine and consequently, the need of producers to protect their typical wines from imitations, which led to the creation of warranty marks linking the wine with the “terroir” where is produced. One of the most important warranty mark is the Geographic Denomination of Origin, issued by the European Union for particularly prestigious wines linked with a specific area of production.

1.2 The micro-climate of “Prosecco di Conegliano e Valdobbiadene DOCG

The case presented in this study refers to a small farm devoted to the production of grape which is processed to become “Prosecco di Valdobbiadene”, named after the specific area where the vines are grown. The area of “Prosecco di Conegliano e Valdobbiadene

DOCG” lies (Figure 1) on the hilly northern part of Treviso province (North-Eastern Italy) and Prosecco has been the Italian 44th wine to obtain the Denomination of Origin from the European Union. Geologically, the zone of Valdobbiadene is originated by raising of seabed and part of the hills formed were eroded by

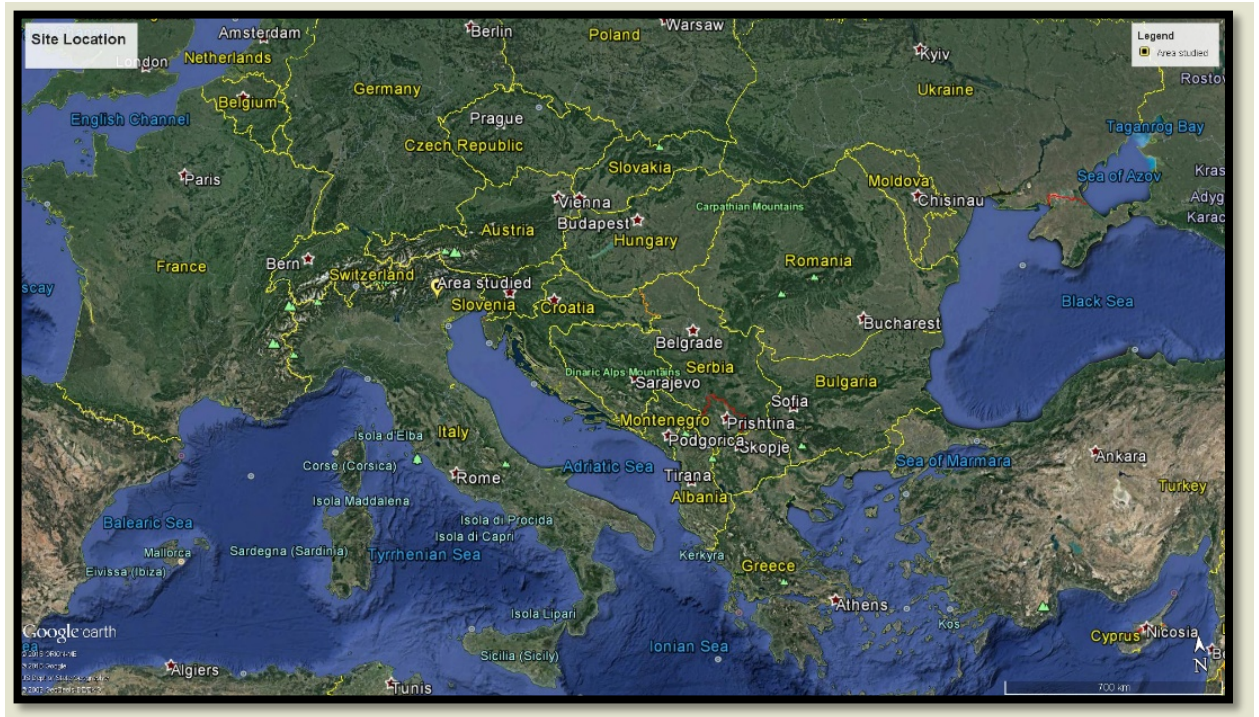


FIGURE 1 - MAP SHOWING THE LOCATION OF THE AREA STUDIED (GOOGLE EARTH)

glaciation. The resulted soils are deep and have high clay content. In other parts of the area where the erosion process did not take place, the soil is less deep and made up of sand and marlstone. The presence of different soils, associated with hills of different slope (gentler in Conegliano and steeper in Valdobbiadene) and aspect has led to the existence of a number of peculiar micro-zones. Furthermore, the position near the pre-Alps and the sea guarantees a stable mild climate with yearly mean of temperatures of 12.3 degree centigrade, in conjunction with a constant breeze which dries the grapes after the rain. Annual rainfall is around 1,250 mm with heavy showers in the summertime. The altitude ranges from 100 to 500 meters above sea level with a good daily thermal excursion and

the hills, stretching from east to west allow the southern facing slope to be cultivated with vines. Is in these peculiar micro-climates that Prosecco and its types as “Glera” or the prestigious “Cartizze” find the ideal conditions to grow.

1.3 Introduction to Precision Viticulture (PV)

Precision viticulture (PV) is based on the fact that there are areas within vineyards that differ and wants to provide means to exploit and measure such variability. The methodologies of precision viticulture are derived from those of precision agriculture (PA), adopted mainly in extensive farming systems. Precision Viticulture is made possible by the combined employment of two important technologies: the Global Positioning System (GPS) and the Geographical Information System (GIS). In addition, a fundamental support is given by both Proximal and Remote Sensing. Researches proved that PA shows to be profitable for high value crops and vine grapes through its transformation process to wine acquire a very high value (Profitt *et al*, 2006).

In brief, PV can be implemented as a cyclical process made of three steps:

- Observation and data collection: this step is performed through either proximal and /or remote sensing. Proximal Sensing (PS) refers to use of instruments which capture information through physical contact with the mean studied, whereas Remote Sensing (RS) aims at collecting information from a given distance.

- Data interpretation and evaluation: the raw data needs to be processed and analysed and this step requires the use of GIS software.

- Implementation or modification of the vineyard management plans according to the information acquired. The information acquired and analysed allow to take action as for instance to changes farming practices.

1.4 Aim of the study

In this study the technologies of Precision Viticulture (PV) will be integrated with Geographical Information Systems (GIS) in order to improve farm management using images acquired with Unmanned Aerial Vehicles (UAV). In particular, the research focus on a small farm with the primary intention to increase the awareness on how the mentioned technologies can be beneficial for farmers.

The research's overall purpose is to give a small but effective contribute in the employment of Precision Viticulture technologies, which can be applied even to small scale farms and can help farmers and agronomists in the decision making process. The main goal is, by acquiring remote sensing data, to improve the knowledge of the variability of vineyards and to measure such variability. This improvement could potentially lead to modification of agronomic practices and in some extent, reduce the farm's costs and/or to improve the quality of the final product, hence getting an increment of the profits.

The specific objectives of the study are:

1. Use two affordable Unmanned Aerial Vehicle platforms as well to types of camera for images collection.

2. Spatially build a 3D model of a vineyard using the Photogrammetry Technique named Structure from Motion (SfM). The goal is to obtain a good estimation of the leaf area index (LAI) of the vineyard by using a relatively inexpensive methodology compared with Laser Detection and Ranging (Lidar). The knowledge of the 3D map of the vineyard can help the farmer to tune the agronomic technique according to the plant structure: for instance, practice like pruning, spraying, fertilizer broadcasting can be fine-tuned knowing the canopy density and consistently allow saving in labour and inputs.
3. Create a vigour map of the area by calculating NDVI/PCD from aerial photographs images. By using an inexpensive Unmanned Aerial Vehicle provided with a consumer modified NIR camera to generate homogeneous maps of the vineyard with the purpose to pursue a differential management.
4. Analyse the Digital Terrain Model and its derivatives as slope and Topographic Wetness Index to study the presence of clusters of homogeneous zones.

CHAPTER 2 – LITERATURE REVIEW

2.1 Introduction

Amongst many definitions that could be given, Viticulture could briefly be outlined as the science of vine growing and grape production. The vine as a crop was grown by the human being since the ancient time and wine has been a renowned product consumed in all the ages. The trend of the modern wine industry moves towards a demand of quality wine from the final consumer perspective and a reduction of the costs from the producer's point of view. This fact is proven frequently by the higher price paid by many consumers for quality wine and by the marketing oriented towards a differentiation of the product in the offer platform. Different studies have proven that the increment of the yields can be detrimental for the final product quality. Hence, the producers associations have developed a number of protocols which tend to limit the production of grapes per hectare in order to maintain an adequate quality of the wine. On the other hand, this limitation has led to the necessity to optimize the inputs in a bid to reduce the costs. This fact is proven to be even far more important if we consider realities in which the mean farm size is 5 Ha, as in the north eastern Italy and Treviso Province. Notwithstanding, to reach these objective new tools needs to be unfolded in order to improve the knowledge of the spatial and temporal variability *in situ* and accompany the growers in the decision making process, for instance by allowing to optimize the inputs, also with the scope to improve the sustainability of the agricultural system as a whole.

Is in this background that viticulture and Geographical Information Systems (GIS) has found a tight link, being GIS an important tool that adds information regarding the vineyard's spatial variability. Aided by the developments in the remote sensing through

the availability of satellite imagery, airborne imagery and Unmanned Aerial Vehicles imagery, there are so far untapped possibilities in the sector of GIS services for viticulture.

2.2 Spatial variability in the vineyards

Vineyard variability can be intended both in spatial and temporal meaning and the first occurs as a result of unequal topography, soil features, farming practices, plant health conditions and climate. Temporal variability mostly depends on changing weather conditions (either seasonally or in different years) or appearance of pests and diseases (Profitt *et al.*, 2006). The spatial variability inside vineyards has always been a problem difficult to determine quantitatively and to manage. This variability implies both vegetative and productive differences which can heavily affect the final product (the wine). Actually the technology has made available tools as infrared sensors which allow to quantify in detail such variability, making possible to develop an in-farm viticultural and oenological management based on maps which express visually the vegetative state of the vineyards (Rossetti *et al.*, 2011).

The importance of quantifying the variability of vineyards even in small farm is stressed by Green *et al.*, (2012) who highlighted the opportunity to collect free agro-climatic data as temperatures, rainfalls, humidity and the usefulness to display this information visually.

In a case study he used the Digital Terrain Model and Digital Surface Model derivatives and joined it with soil properties as PH and soil humidity to analyse intra-vineyard variability through cluster analysis. The findings in the specific case are that the size of the vineyard was too small to depict any appreciable variation and that the diversifying

factor was related with insolation as the shadowing between plants might generate negative effects.

2.3 Overview of Unmanned Aerial Vehicles (UAV) image acquisition in PV

Unmanned Aerial Vehicles (UAV) are small size aircrafts remotely operated which have found a diverse range of applications. One of the most promising field of application of UAVs equipped with different sensors is in the realm of Precision Agriculture (PA) for yield mapping, creation of vigour maps, monitoring of vegetation stress, plants' disease detection. Their applicability has proven to be cost effective as they can provide hyperspectral images and RGB photographs at a considerable minor cost compared with other form of remote sensing (e.g. satellite and airborne imageries). Moreover, an advantage of UAV is that they can provide quality images even in a cloudy day and that their high flexibility flight program permits repeatedly to collect images of plants at different physiological stages. In spite of the benefits, the shortcomings in the use of UAV are basically related with their platform reliability, sensor capability and lack of standardised procedures to process large amounts of data (Zhang and Kovacs, 2012).

2.4 Vegetation Indexes

Maltese *et al.*, (2014), compared NDVI surveying collected from UAV, aircraft and satellite with the purpose to assess the variability inside the vineyard. The result of the study outlines that the different platforms provided similar results in vineyards with coarse vegetation gradient. The most interested finding of the research was that in heterogeneous vineyard characterized by extreme patchiness low resolution images failed to represent the state of the vegetation. Additionally, a cost analysis study aimed at

determining the feasibility of the use of the three platforms in a context of different farm sizes outlined that the use of UAV was profitable for small vineyards with size less than 5 Ha, while, above the 5 Ha threshold, airborne and Satellite collected imageries proved to be more cost-effective.

2.4.1 Leaf Area Index (LAI)

The Leaf Area Index (LAI), defined as one half of the total leaf area per unit of ground surface area, is a vital crop parameter, important because it allows to modulate different interventions in the vineyards' management. Direct measures methods of LAI are very precise but labour intensive and thus, impractical in the day-to-day management of vineyards. Recent researches have proved that the combination of hyperspectral data and crop surface model can give good results in the estimation of leaf area index, whereas the 2D RGB Orthomosaic showed a lower r^2 (Breada, 2002).

2.4.2 Normalised Difference Vegetation Index (NDVI) and Plant Cell Density (PCD)

In spite of the fact of being used for vineyard zoning (Johnson *et al.*, (2003)), NDVI index has shown, in some research, controversial results (Di Blasi *et al.*). The NDVI is a numerical indicator capable to express the intensity of the vegetation vigour and is related to both health status and leaf area index (LAI).

The NDVI is the ratio of the reflectance in the near-infrared band (NIR, 0.75–0.90 mm) and the reflectance of red in the visible band (RED, 0.61–0.70 mm), as indicated by Krieger *et al.*, (1969):

$$NDVI = \frac{NIR - VISred}{NIR + VISred}$$

Johnson et al., (2003) have proved that NDVI is strongly related to the plant canopy leaf area index (LAI). In fact, chlorophyll strongly absorbs visible light (0.4–0.7 mm) for photosynthesis, whereas the cell structure of the leaves strongly reflects near-infrared light (0.7–1.1 mm).

Consequently, a dense and healthy canopy will provide low values of reflectance in the red region and high values of reflectance in the near-infrared region, which results in high NDVI values. On the other hands, under condition of poor or unhealthy vegetation, the NDVI has a low value. The NDVI of vine leaf area is related to the amount of photosynthetically active radiation adsorbed, hence to vine water status, fruit characteristics, and wine quality.

Plant Cell Density (PCD) sometimes called Ration Vegetation Index (RVI) is an index similar to NDVI and is mathematically represented by the equation:

$$PCD = \frac{NIR}{Red}$$

Is the ratio between the reflectance of the near infrared band (NIR) and the red band with high value for photosynthetically active biomass (PAB) and low for plants with less photosynthetically active. In some research PCD has outperformed NDVI in estimating canopy pruning weights while NDVI gave better results in estimating the anthocyanins fruit content: in any case there are factors influencing the performance of both indexes as Plants and row spacing and vegetation density (Profitt *et al*, 2006).

2.5 Vineyard canopy reconstruction through Structure from motion

Structure from Motion (SfM) is a computer vision technique that has been used in different sectors and it has proved to give good result in the reconstruction of 3D objects: the main advantage of SfM is its low cost, rapidity and capacity of automation particularly

if compared with the Laser Detection and Ranging (Lidar). SfM has been used for topography reconstruction to study coastal system process in order to recreate a DSM of sandy dunes (Mancini *et al*, 2013).

SfM has proven to give results comparable with those provided with Lidar in determining Horizontal and vertical distribution of forest canopy and information on individual trees in areas with relatively low canopy closure. Notwithstanding, SfM underperformed Lidar if employed in condition of dense canopy coverage but still proved to be a very competitive technique for its very low cost (Wallace *et al*, 2016).

In Texas vineyards, SfM was used to create a dense points cloud, then points were classified in ground and non-ground, the latter presumably representing the plants' canopy, in order to recreate the 3D structure of the vineyard. In several locations of the vineyards, the LAI (Leaf Area Index) were measured indirectly and a regression model was put in place in order to estimate the LAI of all the area. However, the statistical analysis showed a low R^2 leading to important justifications in using the SfM for creation of 3D model of the vineyard canopy. Moreover, SfM performed well in comparison with Lidar, let alone the advantage to be a low cost technology that gives the possibility to repeat the measurement over time. SfM main limitation is related with the fact that can be used in small areas (Mathews and Jensen, 2013).

The importance of vineyard's canopy reconstruction is highlighted in different studies and finds the rationale in the fact that a correct knowledge of canopy can help to save inputs: the canopy reconstruction made with Lidar acquired data allowed to calculate the LAI and most importantly the total Leaf Wall Area (LWA): spray adjustment can be done on variable dosage spraying equipment provided with GPS, based on the knowledge of this parameter. LWA represents the area of the canopy measured vertically and can be

accurately estimated acquiring images with Lidar ((Llorens Calveral *et al*, (2011) and Gil *et al*, (2014)).

Sansebastian *et al*, (2015) tried to analyse viticultural zones at whole vineyard scale in big farms and, even though he was able to separate in classes with oenological and agronomic implications, found no correlation between homogeneous zones and quality of wine.

Rossetto *et al*, (2011), developed a software name Enovitis™ which use data provided by remote (through UAV) and proximal sensing to optimize the agronomic practises inside the vineyards: the best positive outcome is that the provided data of a practical economical savings in the case study. Besides, they proved that the vineyard's characterisation through the construction of vigour maps derived from multispectral images collected from a UAV, led to a intra vineyard zonation which allowed a selective harvesting.

Fiorillo *et al*, (2012), investigated the value of airborne NDVI images collected at different vine's phenological stages and quality index of grapes harvested at different dates. The study proved the importance of NDVI as index to differentiate zones of vineyard with different quality. Notwithstanding, the study evidenced the fact that the NDVI significance may vary with the harvesting dates, probably suggesting the existence of different populations inside the cultivar "Sangiovese" vineyard and a different degree of correlation between NDVI and different harvesting time.

Hall *et al*, (2010), studied the variation over time of the correlation between vineyard canopy and both quantitative and qualitative parameters of grape. The main outcomes were the existence of a correlation both of yield and fruit quality parameters and vineyards area and density; however, such correlation was dependent from the vegetation stage of the plants: for instance, the same parameter (i.e. Anthocyanins) had different correlations before and after flowering.

However, in all the studies so far reviewed the applicability of remote sensing technologies as the use of UAV in fragmented vineyards has not been assessed. Fahrentrapp *et al.*, (2015) tried to assess the applicability of such technologies in highly fragmented vineyards in a bid to illustrate potential correlation between NIR/RGB photography and physiological indexes. The results prove that even simple approaches using relatively inexpensive tools can lead to differentiation of canopy's management methods. Notwithstanding, in the specific case, no relevant differences in the quality of the final product with different vineyard management were observed.

Mazzetto *et al.*, (2010), considered the possibility to use proximal sensing in order to determine the plant vigour and the presence/absence of diseases as mildew (*Plasmopara viticola*). The results showed a positive correlation between plant vigour (correlated with NDVI index) and the presence or absence of the disease, which affects heavily the density of the plants canopy. The study also outlined that the combination of NDVI and UCT can allow to identify areas where plants have a reduced plant density because of the disease possibly leading to a system of detection of the diseases.

2.6 Object Based Image Analysis (OBIA)

Object Base Image Analysis (OBIA) is a GIS technique that segments remote sensed images to meaningful image objects, which will be analysed for their texture, spatial, spectral and temporal feature. OBIA basically unifies pixels according to specific algorithms and wants to solve the problems of pixel-based analysis.

OBIA has been used to characterise the canopy of olive trees in orchards through UAV multi-spectral acquired images, applying algorithms that make trees equals to geometric

solids: the study suggests that the method could be used in other woody crops (Torres-Sanchez *et al*, 2015).

In fact, it has been used to identify vineyards from satellite borne images resulting in being able to distinguish among different vine varieties (Senturk *et al*, 2013).

One alternative to the OBIA, proposed by Burgos *et al*, (2015) was to collect the images at high resolution with an UAV and through a Python-based algorithm, derive the Digital Terrain Model. The Digital Difference Model calculated by the difference between the DSM and DTM represents the non-ground and thus the canopy.

2.7 Vineyard zonation

Di Blasi *et al*, (2010) has evidenced the relation between NDVI measured and Practical intervention in the vineyards proving that both proximal and remote sensing can aid the farmer in the decision making process, for instance applying a differentiated pruning intensity depending on the single plants vigour.

Priori *et al*, (2012), in their research combined proximal and remote sensing to map vineyards in order to outline homogeneous zones which in effect gave grapes and wine of different quality. The parameters studied were the soil electrical conductivity measured at 2 different soil depth, the Topographic Wetness Index (TWI) and NDVI extrapolated from multispectral airborne images collected from UAV: the positive finding was a significant statistically difference between harvesting zones which allowed the vinification of wines of different qualities, hence proving the correlation between vineyard zoning and quality differentiation intra- vineyards. However, among the four variables considered, only the soil electrical conductivity (at both soil depths) had a strong positive correlation with the 2 harvesting zones, whereas TWA and NDVI showed a smaller correlation.

Profitt *et al.*, (2006) observed that the best results in terms of vineyard zonation with the purpose of obtaining wines of different qualities was collecting image at the stage of veraison: the statistical analysis of NDVI maps from image collected at this specific phenological moment provided meaningful separation of homogeneous zones. Furthermore, in a 3.3 Ha plot of Cabernet Sauvignon analysis of Plant Cell Density (PCD) map showed zones with less vigorous and others with more vigorous plants. The images were collected before pruning allowing to a differential management of the plants based on their vigour and allowing a consistent saving of labour cost.

Cluster analysis of local slope, Topographic Wetness Index and cumulative moisture in two Italian vineyard along with hydrological models were used to predict grape yield and wine quality even if the results were not the same for both the sites (Costantini *et al.*, 2009).

CHAPTER 3– METHODOLOGY

3.1 Important premise

It is important to notice that the methodology governing the study has some strength as well some weakness. The positive aspect of the research is that it serves the practical scope to prove the benefits of acquiring information using UAVs as a tool in precision viticulture: in the short term benefits could be the possibility to apply differential management of homogeneous zones. This need was clearly explained by the owner of the farm. During the data collection a “list of needs” was filled by the farmer, who pointed out that, due to the farm location on hilly areas, irregularity of the plots and intra-plot lack of uniformity of plant canopy vigour, the biggest problem is the intense labour effort in the manual operation, in particular referring to the pruning cost which must be repeated several times over a season. Besides, Is important to notice that this research do not aim at a vineyard zonation in order to select homogeneous zones for producing wine of different qualities: in fact, in order to obtain reliable results data should be collected at the phenological stage of veraison, which normally occurs around the end of August. Nevertheless, the aim is to determine the possibility in a small area of the farm to separate area of different vigour which would require different management allowing the farmer to save time and at the end to reduce the labour cost.

The limit of this study is that due to lack of budget and strict timeframe the indispensable ground truth cannot be performed: some the measurements of physiological indexes as well the combined chemical analysis of both the grapes and wine of the different harvesting zone might add value to the research which, at the moment, is mainly demonstrative. In fact, even if the study will be able to separate different harvesting zone,

it will not be able to prove that such differentiation leads to an effective difference of quality in the wine produced.

3.2 Description of the area studied

The area selected for the study is located on the north-eastern part of Italy and precisely in the village of Santo Stefano di Valdobbiadene (Province of Treviso): the exact location of the site is 45.89 N Latitude and 12.02 E Longitude and the site's area covers 1.950 square meter. The farm cover an area of 8 Hectares scattered in different locations and the size of plots ranging from 3 Ha to 0.02 Ha. This intense scattering of the farm is typical of the area and represents the prevailing model among the farms. Furthermore, the plots lack in uniformity as a result of replanting in different years and in the same plot is not unusual to find plants aging 100 or more years and plants of much younger age (generally 40 years old). The row spacing is 4 meters but as is possible to evince from the images is fairly irregular whereas the plants distance averages on 3.5 meters. The area is irregularly slope (2-10%) and the soil is characterized by being alluvial with a good clay content. The climate is temperate the annual mean temperature (see appendix) is 11.7 degrees the annual rainfall is approximately 1000mm. Form more detailed information about th climatic condition in appendix 1 is possible to find data concerning temperature (maximum, mean and minimum), rainfalls and relative humidity (minimum and maximum). The weather data were downloaded for free from the website www.arpa.veneto.it and are routinely collected from the station located in Valdobbiadene. The vineyard site is one of Prosecco DOCG designated to produce the "Prosecco of Conegliano and Valdobbiadene".



FIGURE 2 - AN EXAMPLE OF THE VARIABILITY: THIS VINE WAS PLANTED AFTER THE FIRST WORLD WAR.

Most of the agricultural practices as pruning, spraying and harvesting are not mechanized and carried out by the owner/farmer, who is aided by casual workers when needed. Additionally, the owner does not keep a comprehensive record of the vineyard including spatial information.



FIGURE 3 - MAP SHOWING THE LOCATION OF THE AREA STUDIED



FIGURE 4 - LOCATION OF THE AREA STUDIED IN DETAIL, ENCLOSED IN THE RED POLYGON.

Despite the rains of the weeks prior to the images capturing the vineyard appeared in good condition and the plants did not show apparent signs of diseases or stress.

3.3 Description of equipment used to collect and process the data

In this study two Unmanned Aerial Vehicles (see table below) were used in a bid to test their respective easiness to operate from a beginner perspective: each of them consists in a remotely controlled quadcopter, a gimbal necessary to stabilise the sensor and a camera to acquire the images. The images were stored in a memory card chosen for the ability to record images in rapid sequence.

No.	UAV	Gimbal	Camera	Comments
1	DJI Phantom 2	Zenmuse H3-3D	GoPro Hero 3+ Silver Edition	IGotU geotagger was attached to the UAV
2	3D Robotics IRIS +	Tarot 2D	Mapir Survey 2 NDVI model	

TABLE 1 - EQUIPMENT EMPLOYED TO ACQUIRE THE IMAGES

3.3.1 DJI Phantom 2 with Zenmuse H3-3D Gimbal and GoPro Hero 3+ silver edition

Phantom 2 (P2) is a quadcopter manufactured by the Chinese company DJI. P2 is the second version of the Phantom series and has some important modification over the previous one, aimed at improving on-fly safety. The reliability of its built-in Naza autopilot show changes compared with the first version of DJI Phantom: in addition to the compass performance an intelligent battery allows to know the status of the charge and a return to launch switch in case of runaway or loss of control of the quadcopter. In case of low battery level the drone returns to its launching point automatically avoiding

dangerous situations of fly-away. The version used in this was provided with a First Person View (FPV) Blackpearl monitor (with Fatshark antennas): this is a 7 inches screen connected via radio with the drone where is possible to have the view from the camera mounted on the Phantom. Moreover, a DJI iOSD On Screen Display (OSD) shows directly on screen telemetry data as flight altitude, coordinates and battery status. However, the iOSD mini version provided with this Phantom does not record the telemetry data in a memory card, thus an external GPS logger was used to record the flight path to properly geotag the images.

The P2 used in this research mounted a Zenmuse H3-3D gimbal necessary to stabilise the camera and get still images when the UAV flies. The H3-3D gimbal is a 3-motors consumer version which retains most of the capability of the professional level Zenmuse gimbals. It supports different GOPRO cameras as well other action cameras.

In this specific case the camera used was a fisheye lens lightweight (85gr) GOPRO Hero 3+ silver with 10 Megapixel resolution and the RGB images (in JPG format) were stored in a memory card Lexar microSD 1000x.

One important aspect to notice is that P2 does not store the telemetry data hence is not possible to geolocate the images acquired. In order to solve this problem a small GPS logger (IgotU) was tied in one of P2 legs: it is a lightweight device (20 grams) which record the coordinates in its own memory. The log file can be downloaded and used to geotag the images.

UAV	DJI Phantom 2	3D Robotics IRIS +
<i>Weight (Battery and propellers included)</i>	1000 grams	1282 grams
<i>Max flight speed</i>	15 m/sec (Not recommended)	11 m/sec
<i>Diagonal Length</i>	350 mm	550 mm
<i>Flight time</i>	25 mins	15-20 mins
<i>Payload capacity</i>	300 grams	400 grams
<i>Supported battery</i>	DJI Smart Battery	5100 mAh 3S
GIMBAL	Zenmuse H3-3D	Tarot 2D
<i>Number of axis</i>	3	2
<i>Weight</i>	168 grams	200 grams
<i>Control angle range (degrees)</i>	Tilt axis control -130 +45 in the 3 axis	± 45 (roll) -135 +90 (tilt)
<i>Camera supported</i>	GOPRO 3 and 3+	GOPRO
CAMERA	GoPro Hero 3+ Silver	Mapir Survey 2 NDVI
<i>Type</i>	Fisheye	Frame
<i>Resolution</i>	10 MP	16MP
<i>Bands</i>	Red, Green, Blue	Red (660nm) + Near InfraRed (880 nm)
<i>Weight</i>	74 grams	64 grams

TABLE 2 - MAIN CHARACTERISTICS OF THE EQUIPMENT USED TO COLLECT THE IMAGES



FIGURE 5 - DJI PHANTOM 2 MOUNTING THE GIMBAL. BELOW IS POSSIBLE TO SEE THE GOPRO CAMERA (LEFT) AND THE GEOTAGGER (RIGHT).



FIGURE 6 - 3D ROBOTICS IRIS+ MOUNTING MAPIR NDVI CAMERA.

3.3.2 3D Robotics IRIS+ with Tarot 2D Gimbal and Mapir Survey 2 NDVI camera

IRIS+ is a quadcopter manufactured by the American company 3d Robotics which offers some advantages over the Phantom 2: the most important one is that is provided with a Pixhawk autopilot that allows to save in a memory card the flight data including flight altitude and GPS location of the aircraft. Secondly, it offers interesting options

for the beginner as a completely programmable flight path and the follow-me function: both this functionality might be interesting for operators with little experience in flying UAVs and IRIS+ can take off, fly, and land almost autonomously once the flight path is programmed through some free software (Andropilot or DroidPlanner to name just a few) installable in any Android device. However, the major disadvantage of this UAV is the battery duration (approximately of 15 minutes) slightly less than the Phantom 2 (typically 20 minutes).

IRIS + as the P2 does not come out of factory with an already installed camera and gimbal and lets the user the possibility to choose, although the choice is limited by the payload

In this study IRIS+ mounted a 2 axis Tarot Gimbal used to stabilise a MAPIR Survey 2 aerial Mapping camera NDVI model.

MAPIR Survey camera NDVI can collect images at 16MP resolution with its non-Fisheye lens and has exactly the same dimension of a GOPRO 3+, although weighs only 74 grams. The camera can acquire images in RAW+JPG as well as JPG format and has a dual-band filter that captured reflected Red light in the RGB sensor's red channel and reflected Near Infrared light in the RGB sensor's blue channel. Thus, this single camera can acquire images in both Red and Near InfraRed (NIR) band; such images can be used to compute vegetation indexes as NDVI or PCD, though the contrast in the resulting index image will not be as "accurate" as using the separate Red and NIR camera models.

The camera stored the images in a memory card Lexar microSD 1000x.

The images from this camera can be processed in any ortho-mosaic generating program.

This NDVI model sees both Infrared 850nm and Red 650nm light. The images from this camera are commonly calibrated into an index image and then a coloured lut is applied to show contrast between healthy and poor health vegetation.

The Survey2 cameras have a faster interval timer: 2 seconds for JPG mode and 3 seconds for RAW+JPG mode.

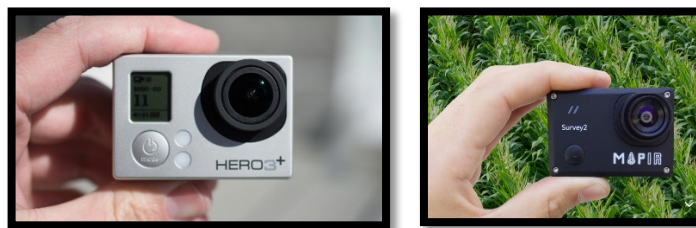


FIGURE 7 - GoPRO HERO 3+ (LEFT) AND MAPIR SURVEY 2 NDVI (RIGHT)

3.3.3 Description of the software and hardware used in this research

The software that will be used in the research is mentioned in the table below:

Company/developer	Software	Specifications Extension	Website
<i>IGotU</i>	TripPC		CD-rom provided with device
<i>3D Robotics</i>	Mission Planner	Free software	https://3dr.com/about/software/
<i>Friedmann Schmidt</i>	Geosetter	Freeware	www.geosetter.de
<i>Agisoft</i>	Photoscan		www.agisoft.com
<i>Pix4D</i>	Pix4D Mapper Pro		www.pix4D.com
<i>Qcoherent</i>	LP360	Advanced level	www.qcoherent.com
<i>PCI Geomatics</i>	Geomatica	Focus	www.pcigeomatics.com
<i>ESRI</i>	ArcGis	Spatial analyst, 3 D analyst, spatial statistics	www.esri.com
<i>Trimble</i>	eCognition developer	QuickMap Mode	www.ecognition.com

TABLE 3 - SOFTWARE USED IN THIS RESEARCH

The hardware employed for all the analysis was a PC laptop quad core Intel i7 with 16 GB Ram: even with this relatively high configuration the processing time, in particular with Agisoft was considerably long.

3. 4 Data acquisition

3.4.1 Ground Control Points (GCPs) and methodology proposed to measure the coordinates

In order to properly georeference the images four Ground Control Points were placed and distributed across the area studied, as we can evince from the figure 8.

It is important to notice that the coordinates of ground control points should be as more precise as possible and the centimetre level accuracy is possible only employing a RTK differential GPS system: normally this setup consists of 2 GPS devices, one of them fixed (not moving) acting as a base and one movable acting as a rover. This kind of devices are typically used in the professional surveying and are very expensive to buy or rent.

In the recent years a number of low cost RTK GPS systems have been proposed: normally they rely on inexpensive chipsets and open source software and they are not ready to use as they need technical knowledge to be mounted and configured. The one proposed in this study is Navspark NS-HP which was supposed to be used as a rover: within three kilometres (in Valdobbiate) from the site there is a public GPS station, which could serve as a base sending the corrections via internet to the rover. Nevertheless this solution, even if interesting could not be pursued because of the problems encountered in the hardware setup. Hence, the four Ground Control Points coordinates were measured with a conventional non RTK GPS Receiver Garmin GPS 60.

The table 4 below illustrates the coordinates of the GCPs and their accuracy, where the figure 8 shows the spatial distribution on the map.

	Label	Type	X [m]	Y [m]	Z [m]	Accuracy Horz [m]	Accuracy Vert [m]
4	1	3D GCP	269482.004	5086118.519	211.192	0.020	0.020
6	2	3D GCP	269539.132	5086135.907	214.972	0.020	0.020
5	3	3D GCP	269483.067	5086113.494	210.488	0.020	0.020
6	4	3D GCP	269474.130	5086142.075	209.949	0.020	0.020

TABLE 4 – GROUND CONTROL POINTS COORDINATES.



FIGURE 8 – POSITION OF THE GROUND CONTROL POINTS ON THE MAP.

The markers consisted in 3 yellow non-reflecting pieces of plaster on top of the poles of the trellis and furthermore, the corner of the building located beside the area studied was used as a fourth point.

The small amount of Ground Control Points was chosen considering the limited extension of the study area. The plastic material used was easily recognisable from photos taken at

an altitude of thirty meters. However, it was more difficult to distinguish it in the red-Nir images.



FIGURE 9 - ONE OF THE YELLOW PLASTIC WRAPS USED TO VISUALISE THE GROUND CONTROL POINTS ON THE IMAGES

3.4.2 Images collection

As we can evince from the table 5, The RGB images were collected on 18th June 2016 while the Red-Nir the next day due to adverse climatic conditions (rain) which did not allow to fly both the UAVs the same day. The light conditions were not ideal tough as the data were collected at 10.00 am (RGB images) and 5.00 pm (Red-NIR) with a partially cloudy sky. Is common practice to acquire images at midday in sunny days as this would reduce the possibility of canopy shadowing effects.

Images (band)	Date	Time	Weather	Flight altitude
RGB	18-06-2016	10 am	Sunny	30
Red-Nir	19-06-2016	5pm	Partly cloudy	30

TABLE 5 - IMAGES TIME COLLECTION

Both the images were supposed to be acquired pointing the camera downward at the nadir, however a setting problem with Tarot Gimbal allowed collection of only oblique Red-Nir images. As we will see latter this problem affected heavily the outcomes of part of the project. The flight path for both the UAVs was set at an altitude of 30 meters above ground in two series of sinuous flights orthogonal to each other. The speed for both the drones was set manually at around 5 m/sec and the image acquisition took respectively 20 minutes for RGB and 5minutes for the red-NIR. The cameras were triggered to take pictures in JPEG format at intervals of one second and the photographs taken during take-off, landing and when the UAV was not flying at the proper altitude were discarded.

A total number of 1263 RGB bands and 202 Red-NIR bands images were acquired.

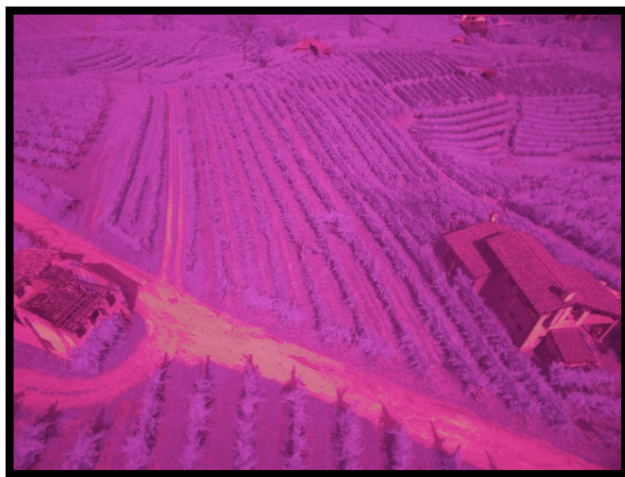


FIGURE 10 – OBLIQUE IMAGE OF THE VINEYARD IN THE RED - NIR BANDS.



FIGURE 11 - IMAGE OF THE VINEYARD COLLECTED IN THE RGB BANDS. IS POSSIBLE TO DISTINGUISH THE DISTORTION CREATED BY THE FISH-EYE LENS.

3.5 Image pre-processing

3.5.1 Introduction

The image pre-processing mainly consisted in assigning a coordinate to each image, as both GoPro and MAPIR camera are not GPS capable and do not assign a GPS location to the photographs. The geotagged images were then sorted with the purpose of choosing the best images for processing.

3.5.2 Geocoding the images

Considering the different UAV setups the images were geocoded using two different software:

1. The images collected with GOPRO camera were synchronised initially with TripPC software provided by IgotU GPS logger (<http://www.i-gotu.com/>).
2. The images acquired with MAPIR CAMERA were geotagged using Mission Planner, the free software provided with 3DR Iris+, which allows in a three-steps process to pair the images with the flight GPS coordinates.

Due to the discrepancy between the cameras' triggering time (set at 1 shot per second) and the GPS coordinates capture both the groups of images resulted slightly misplaced and were necessary a manual correction of the geolocation using a freeware software named Geosetter.

3.5.3 Selecting the best images

The geotagged images were sorted according to 4 criteria:

- 5 All those taken at take-off and landing time were obviously discarded.
- 6 The images showing scenes out of the area studied were discarded.
- 7 The blurry images were discarded as well.
- 8 Finally, images showing exactly the same scene were also discarded.

The image selection narrowed the choice to 27 RGB images and 44 Red-Nir images.

3.6 Image processing

3.6.1 Building the 3D model of vineyard using Structure from Motion (SfM)

The methodology used to build the vineyard 3D model was derived by the study of Mathews (2013).

Structure from Motion (SfM) is a Photogrammetry technique in which a certain number of RGB images taken from different angulation are overlapped in order to recreate a 3D model of physical objects. The points created from the technique have 3 dimensional

information (x, y and z coordinates) and recreate a “Points cloud” in which the additional information of colour is added (Mathews, 2013).

One of the biggest problem of SfM is that is hard to connect the different photographs together due to the high uniformity of green canopy which creates a continuum with the green lawn growing between the vines’ rows. However, the lawn between the vineyards rows was mowed some days before the image collection and left to dry on the field: the dried grass assumed a slight brown colour which permitted to visually differentiate it from the vines canopy.

The images were processed with Agisoft Photoscan in 2 separate chunks, one for the RGB bands images and one for the Red-Nir ones: the decision to not process the images together is explained by the fact that images were collected with two different cameras possessing different specifications and this could introduce noise to the model construction.

3.6.2 RGB Image processing with Agisoft Photoscan

The geotagged images were loaded in Photoscan and whilst the GoPro and its specifications were recognised automatically by the software, for Mapir camera was necessary to input it manually. In any case even for GoPro the fisheye lens correction was set manually as the software did not “see” this important feature.

The images were loaded separately in 2 different chunks and the Ground Control Points coordinates were also added.

The second step was the images alignment selecting the highest accuracy option, even though this selection increased consistently the alignment time. The pair preselection was set in order to have the images overlapping base on their location. Once cameras

alignment was completed Photoscan offered to build the point cloud, a step which involves feature points detection and matching.



FIGURE 12 - POINT CLOUD OBTAINED FROM THE RGB BAND IMAGES COLLECTED WITH GOPRO CAMERA.

Once the process was finished a dense high quality point cloud was built and at this step, images were depth filtered to remove outliers between the points. This process was time consuming for both the chunks taking several hours each.

The dense cloud was used to build the 3D model of the vineyard using interpolation option in order to avoid some hole in the model, due to poor overlapping among images.

Photoscan offers the interesting option to separate the ground from non-ground points and, once the process is completed, is possible to build both a separate Digital Terrain Model and Digital Surface Model.

Subsequently, Digital Surface Model (DSM) and Digital Terrain Model (DTM) were rasterised from the dense point cloud.

The last step was the construction of a high resolution orthomosaic based on source photos and Digital Surface Model.

The dense point cloud was classified in Photoscan to separate ground points from non-ground: the seconds are composed by the low points (noise) and the others representing the canopy feature. Albeit this process was automatic the major problem was importing the separated point cloud as a las file in ArcMap for further analysis as seems that ArcMap cannot recognise such classification. A successive attempt to classify the points cloud with Qcoherent LP360 (advanced version) was also not successful as LP360 requests to project the las file. The projection was performed with define projection tool in ArcGis but the projected file resulted to be geometrically distorted and thus not useful for further analysis.

3.6.3 Red-Nir Image processing with Agisoft Photoscan

The Red-Nir images were also processed with Photoscan to obtain dense cloud, Digital Surface Model, 3D model and orthoimage. The procedure were the same of the RGB apart the camera settings, which were obviously different. As we will see latter the result where not ideal and because of this reason the same images were processed also with Pix4D Mapper.

3.6.4 Red-NIR Image processing with Pix4DMapper

Pix4Dmapper is a software with similar capabilities than Agisoft Photoscan and offers the possibility to get to the final results in fewer steps. Basically it asks to load the georeferenced images, to set the ground control points, to tie the images with the GCPs and with one-click button the process starts: there are almost no options to choose and the Graphic User Interface (GUI) is very much plug-and-play. As a result of it, densified point cloud, 3D textured mesh, raster DSM and orthomosaic were generated. The advantage of Pix4Dmapper over Agisoft Photoscan is that it recognises Mapir camera Survey 2 specification and avoids to set the camera model parameters.

However, the outcomes were not satisfactory, probably as a result of the poor quality source images: due to this fact only some output from Photoscan will be showed in the results chapter, while the outcomes of the processing with Pix4D will be omitted.

3.6.5 Creation of Digital Difference Model (DDM)

The RGB Digital Surface model were imported in Focus Geomatica: this piece of software allows to obtain a DTM almost automatically and to filter it in order to close eventual pits or remove bumps. A shapefile polygon enclosing the area studied was used to clip it from the rest of the context (see figure 13 below).

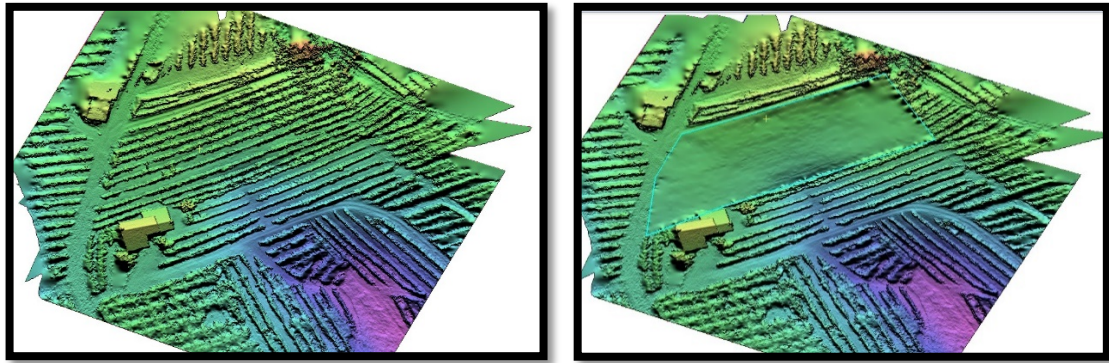


FIGURE 13 - DIGITAL SURFACE MODEL (LEFT) AND DIGITAL TERRAIN MODEL (RIGHT) OF THE AREA STUDIED. THE SECOND WAS CREATED ALMOST AUTOMATICALLY USING THE SOFTWARE GEOMATICA.

The two files were imported into ArcGis and the DDM was obtained with the raster calculator as follows:

$$\text{DDM} = \text{DSM} - \text{DTM}$$

The DDM represents only the vineyard canopy of the area studied.

3.6.6 Derivatives of Digital Terrain Model (DTM) and preparation for cluster analysis

The DTM of the area studied was clipped in ArcMap to isolate it from the rest of the map by using the clipping tool. Subsequently, the derivatives of DTM were calculated by using the ArcGis 3D analyst extension tools: in this way were obtained rasters of slope, aspect, curvature. One problem encountered at this stage was the fact that the distances were expressed in degrees (the maps were not projected) and a Z-factor (in meters) was applied to adjust the unit of measure according to the latitude: for 45 degree latitude the Z-factor is 0.00001171.

Furthermore, the topographic tools were downloaded from ESRI website and Topographic Wetness Index (TWI) was computed. This index is calculated according to the formula:

$$TWI = \ln\left\{\frac{(FA + 1)}{\tan\left((S) * \frac{3.14}{180}\right)}\right\}$$

Where FA is the flow accumulation and S is the slope.

Basically, the denominator represents the local upslope area draining from a certain point for unit of contour, whereas the numerator indicates the slope in radians.

The knowledge of TWI is very important in viticulture as it is highly correlated with soil depth, organic matter content, phosphorous content and percentage of silt.

Additionally, the DTM served as a base raster to calculate the solar map, which expresses the insolation over a certain location. The output is a group of raster maps in which each pixel has a value representing the insolation (in watt hours per square meters): the solar map was computed considering a vegetative period of the vines between April and October. The tool used for this computation was Area Solar Radiation (Spatial Analyst extension).

To perform cluster analysis were performed on DTM, Slope and TWI. The raster files were reclassified by using the spatial analyst reclassify tool in nine classes. The next step performed was the conversion of reclassified raster to polygons. The zonal statistic (a spatial analyst tool) was then applied to the polygons in a bid to calculate the mean value for every polygon. The raster files were again reclassified and converted to polygons to be subjected to cluster analysis.

3.6.7 Vineyard canopy separation with eCognition

The orthomosaic generated from the RGB images was used to separate the vineyard canopy from the ground using Trimble Ecognition developer. Previously, the area studied were clipped from the rest of the context: in order to do so the raster of orthomosaic were converted to vector polygons and then clipped with the polygon representing the area studied. The vector was reconverted to raster and then imported in eCognition.

In eCognition the RGB Orthoimage were first segmented and pixel were grouped according to criteria of scale and colour: the process is iterative and 4 subsequent segmentation were necessary to get acceptable result (figure 15). Multiresolution segmentation (figure14) allows to obtain homogeneous vectors from an image. The segmented layer was then classified following the nearest neighbour algorithm in a bid to separate the vineyard's canopy from the ground and classification was based on colour and texture. The nearest neighbour classification allows to get samples from the feature classes and to define a "positive" class (in this case the vineyard's canopy) and a "negative" class (the ground). The class "canopy" was then exported as in ArcGis for visualisation.

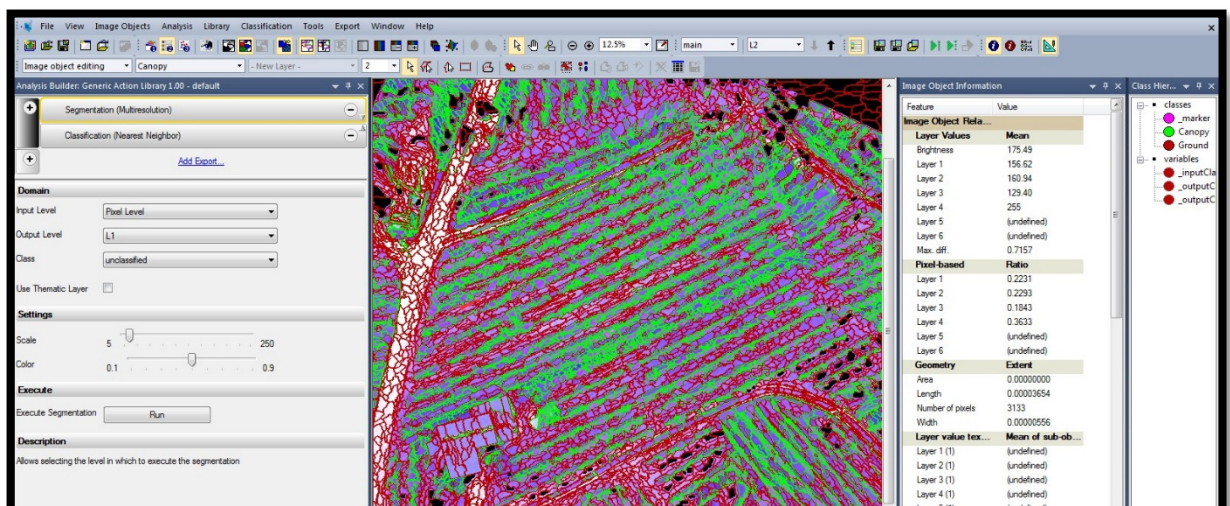


FIGURE 14 - VINEYARD CANOPY SEGMENTATION IN ECOGNITION

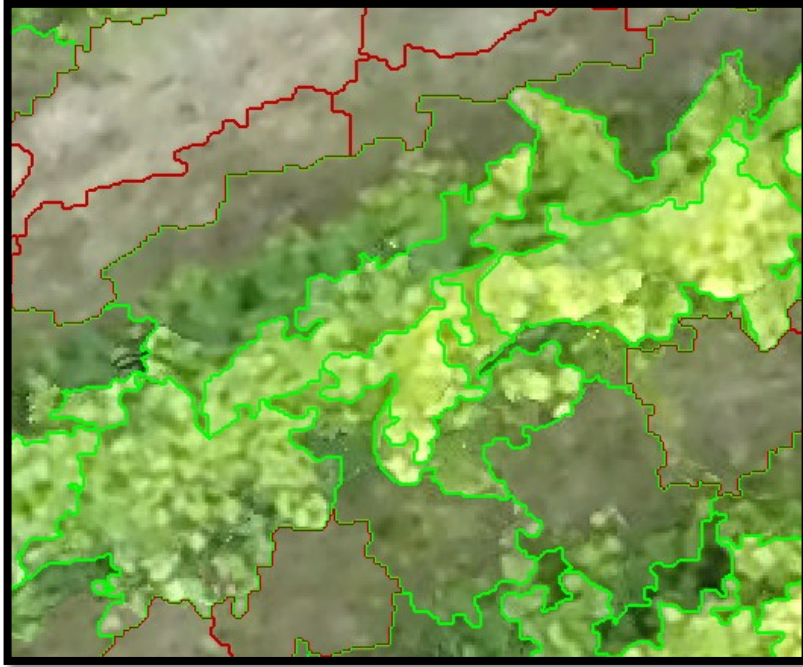


FIGURE 15 - DETAIL OF THE SEGMENTATION PERFORMED WITH ECOGNITION

3.7 Cluster analysis

Cluster analysis was performed to establish the presence of any difference in the parameters on the area studied, which could allow to a differential management of the canopy. Is important to notice that the cluster analysis was performed for brevity only on DTM, slope and Topographic Wetness Index.

Cluster Analysis use basic global statistic to determine if there are clusters. The second steps is to determine critical bandwidth and use iterative process to identifying scales of maximum clustering.

The cluster and outlier analysis (Anselin Local Moran's I) identifies statistically significant hotspots, cold spots and spatial outliers. A positive value for I indicates that a feature has neighbouring features with similarly high or low attribute values; this feature is thus part of a cluster. A negative Moran I value indicates that a feature has neighbouring

feature with dissimilar value and this feature is an outlier. In either instance, the p-value for the feature must be small enough for the clusters or outlier to be considered statistically significant.

The layers positive for Moran I were analysed with the grouping analysis tool: this tool basically groups features based on feature attributes using the k- nearest neighbour as a spatial constraint. The implementation of this constraint requires that to be part of the same group a feature must border with another belonging to the same group. The relationship among neighbours is based on the nearest k-feature. K is represented by an integer value.

The clusters represent homogeneous groups sharing similar values for a given feature.

CHAPTER 4 – RESULTS

4.1 Introduction

This chapter outlines the results obtained from the images processing and analysis explained in the methodology section. It is important to notice that the maps presented in this section represents the situation of the precise moment when data were collected and no temporal variability was taken into account. Notwithstanding, some index as DTM TWI and solar radiation can be considered not temporally mutable. Maps of the vineyards in 4 wavelength, densified points cloud, 3D model, Digital Surface Model and Orthoimage are here presented. In addition, maps of the derivatives of DTM as Slope, Aspect, TWI and Solar radiation are also exhibited. Results of cluster analysis on DTM, Slope and TWI are shown in conjunction with graphics and tables. The results of the elaboration of the Red-NIR bands images are included, although this will give little significance in the analysis. Due to the problem of compatibility between Photoscan and ArcGis the maps presented are not projected.

4.2 Image processing results

Is important to notice that the data provided here are based on calculation made automatically by Agisoft Photoscan for all the area and not just for the area studied. The photos alignment process performed by Photoscan was successful and both 27 RGB images as well as 44 Red-NIR were properly aligned. As a result of that, the (unclassified) point cloud elaborated had 26,069 (RGB band) and 20,090 (Red-Nir band) points and as we can see from the figure 15 and 18 below the outcomes are meaningful, showing clearly

the vineyard' rows, the external road and some feature as the building bordering with the area studied.

IMAGE	RGB	RED-NIR	Difference %
Images processed	27	44	+62%
Tie points (number)	26,069	20,090	-29%
Dense cloud (number)	33,331,996	13,733,525	-242%
3D model (Number of faces)	6,654,112	2,735,168	-243%
Digital Surface Model (Resolution)	1.13 cm/pixel	0.57 cm/pixel	+50%
Orthomosaic (Resolution)	1.13 cm/pixel	0.57 cm/pixel	+50%

TABLE 6- OUTCOMES OF THE IMAGE PROCESSING PERFORMED WITH AGISOFT PHOTOSCAN FOR BOTH RGB AND RED -NIR IMAGES.

Albeit the number of points was only 29% less for the dual band Red-NIR images, the densification process highlighted a much higher number of points in the RGB band (33,331,996) in comparison with the Red-Nir (13,733,525). This proportion is reflected also in the number of faces of the 3D model, in which we can see a number of faces equal to 6,654,112 for the RGB band and only 2,735,168 for the Red_Nir. The resolution of the Orthomosaic and of the Digital Surface Model was 1.13cm/Pixel (RGB images) and 0.57 cm (Red-NIR).

The dense point cloud for the RGB band images (figure 16) shows a uniformity in the part interested to the study. However, when looked in detail (Figure 17) the area below the plants appears without points: this fact could probably lead to an underestimation of the canopy size. This effect is higher in the dense cloud of the Red-Nir band images in

which, in addition, is possible to notice areas completely without points and distortions in the model (Figure 19).

The 3D model recreated in Photoscan from the RGB images expresses a high level of detail and accuracy even if the level of uniformity changes according to the area (see figures 21 and 22). The model generated from the Red-Nir images as well as Digital Surface Model and Orthoimage (figure 24) appears highly inaccurate and distorted: due to this reason the decision was to use for the analysis only the data derived from the RGB band images.

The Digital Surface Model created with Photoscan was imported in Geomatica: the application Focus allows to derive the DTM from a surface model in few steps. The software allows to close pits and flat eventual bumps and the result can be seen in figures 25 and 26. As we can see the altitude of the area studied range from 210 to 216 meters. The Digital Difference Model, obtained by subtracting the DTM from DSM showed an altitude of the canopy ranging from 1.5 to 2 meters. However, some inaccuracies is visible as we can observe in the graph (figure 27) a slightly negative value.

The slope gradient derived from the DTM (figure 28) appeared to be steeper in the central area and around 6-8% on the eastern and western side.

The Orthoimage (figure 29) evidenced a good reconstruction of the scene but at the western and eastern edge of the field is possible to notice some hole.

The results were not positive for the model constructed from the red-NIR band images: it is evident the presence of areas with “zero value” in which the software were unable to process properly the images (figures 31 and 32).

The canopy was successfully isolated from the background with eCognition software. However, as we can see points in figure 33 (see arrow), there were still non-canopy parts

present (representing the grass between the vines rows) showing the limit of the algorithm used based only on colour and texture.

The topographic Wetness Index (figure 34) derived from the DTM had values ranging from 0 to 0.239.

The figure 35 exhibits the map of the solar analysis: the values (in kwh per square meter) are calculated as a mean of thirteen rasters in which the solar radiation was calculated over a period of 14 days, from 1stApril to 30th Septemeber. Hence, the map's values are the mean of the solar radiation for the vegetative period from April until September.

4.3 Cluster analysis results

The cluster analysis (Figures 36, 37, 38, 39 and 40) revealed a positive autocorrelation (positive Moran I) for the DTM (Moran I= 0.487128) and the slope (Moran I = 0.722621) and negative for the TWI (-0.375502). This data put in evidence the presence of clusters for DTM and slope factor, whereas according to this index the TWI data are dispersed (not clustered).

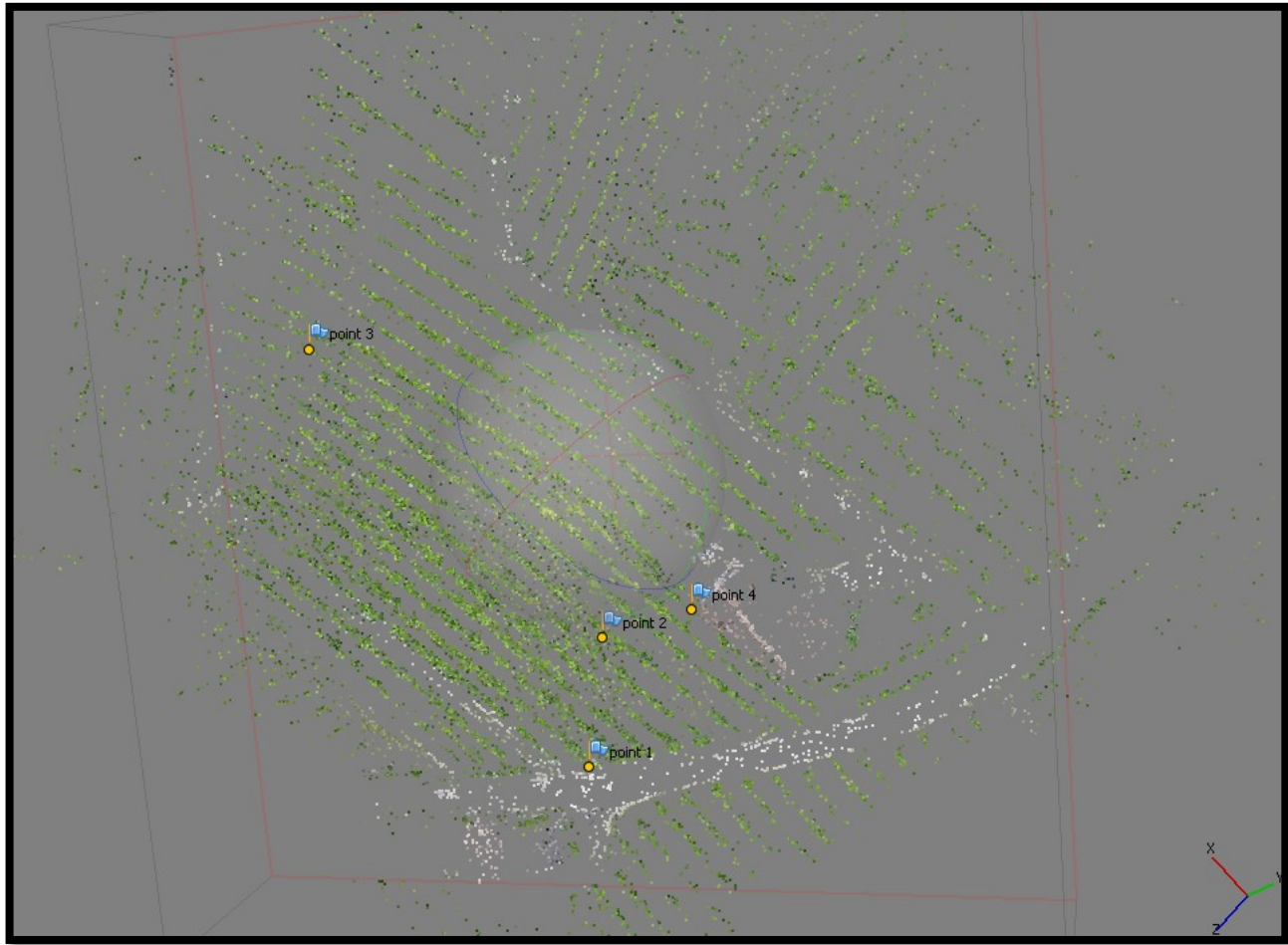


FIGURE 16 - POINT CLOUD FROM RGB IMAGES BEFORE DENSIFICATION. IT IS POSSIBLE TO APPRECIATE THE DISTRIBUTION OF THE GROUND CONTROL POINTS.



FIGURE 17 - POINT CLOUD AFTER DENSIFICATION (FROM RGB IMAGES).

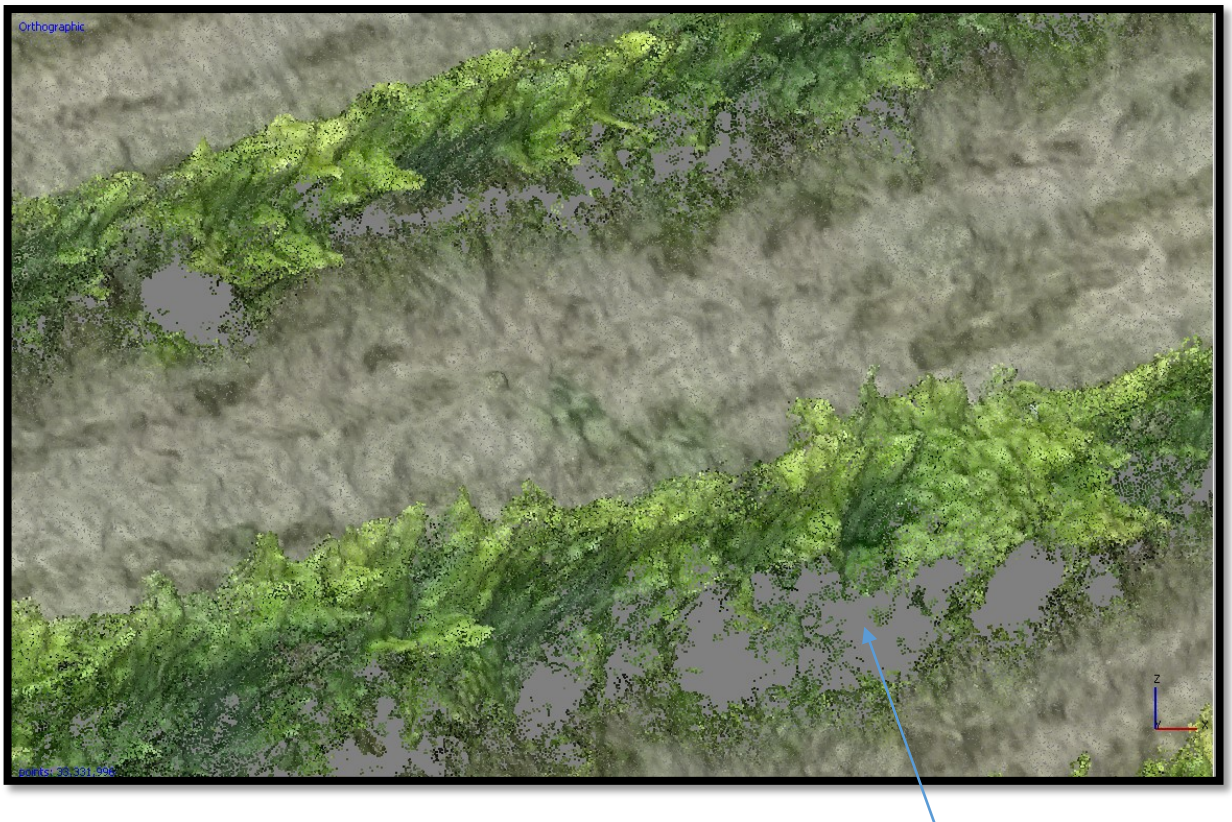


FIGURE 18 - DETAIL OF THE DENSE POINT CLOUD OBTAINED FROM RGB IMAGES.

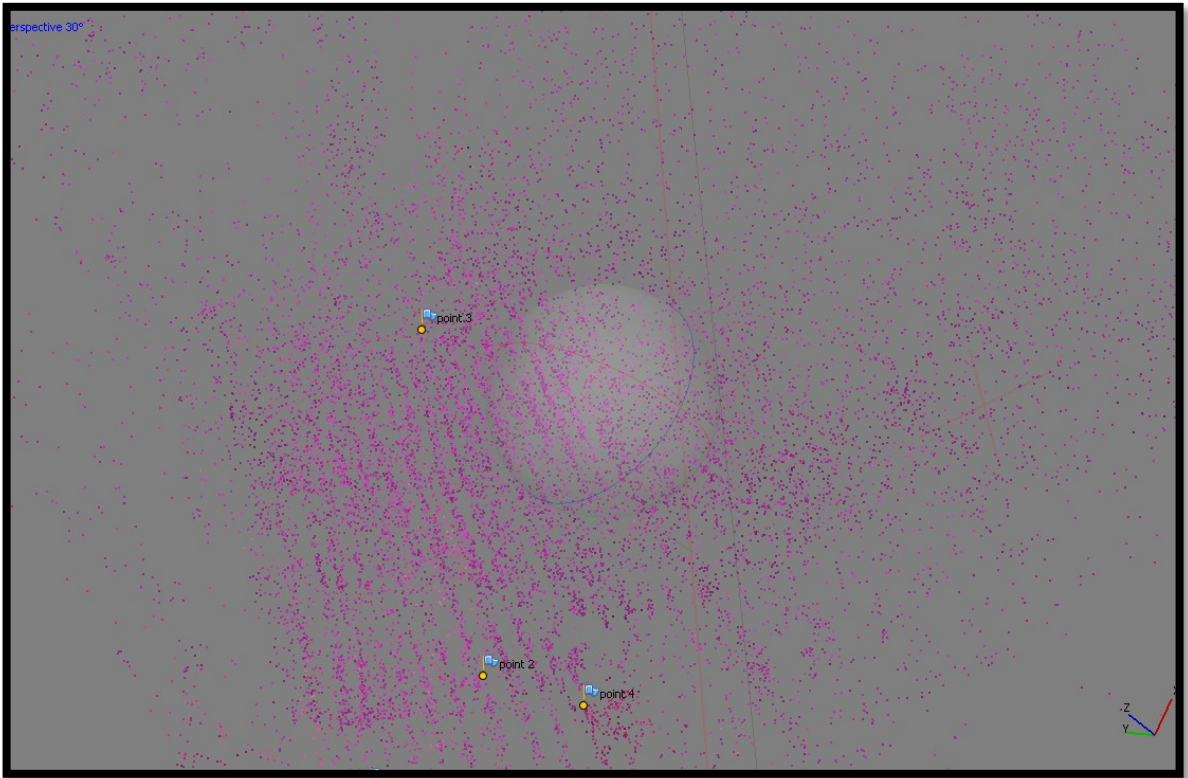


FIGURE 19 – POINTS CLOUD OF THE IMAGES IN THE RED-NIR BAND BEFORE DENSIFICATION

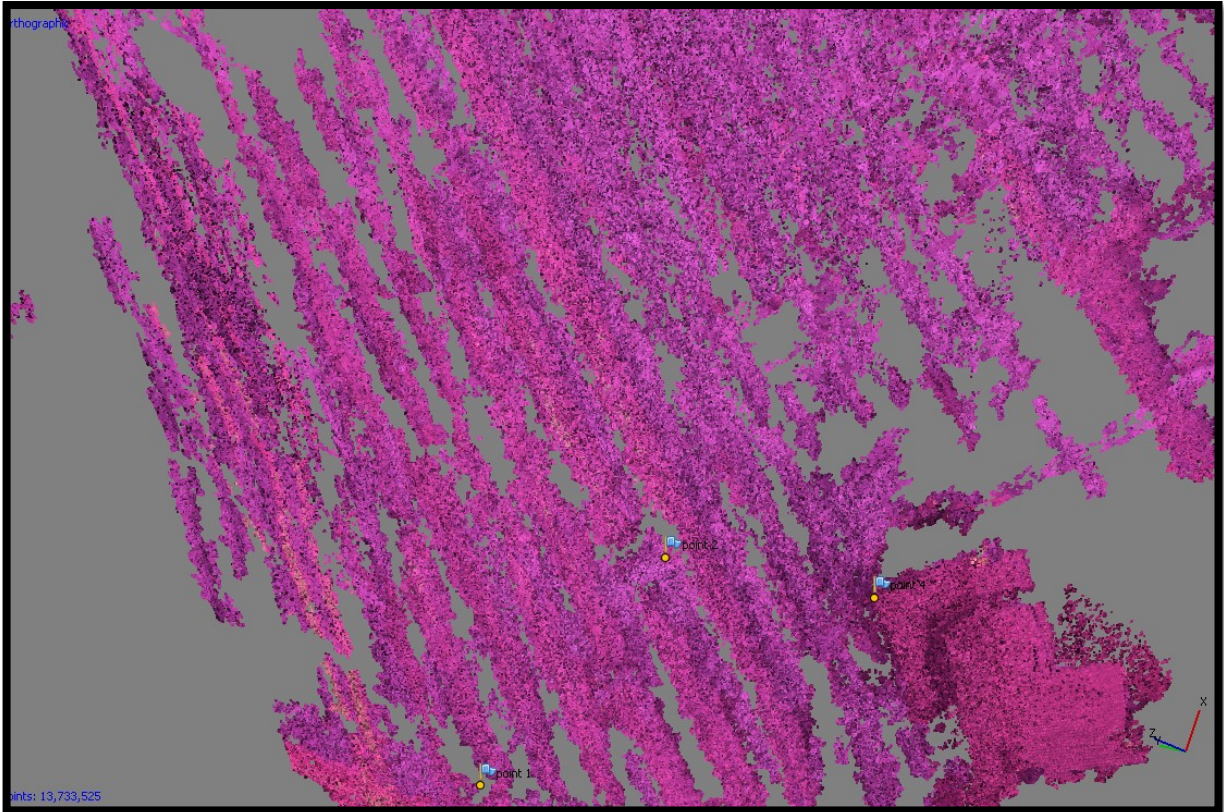


FIGURE 20 - POINT CLOUD AFTER DENSIFICATION OBTAINED FROM THE RED-NIR BAND IMAGES.



FIGURE 21 - DETAIL OF THE CANOPY RECONSTRUCTION FROM RGB IMAGES.



FIGURE 22 - LATERAL VIEW OF THE CANOPY RECONSTRUCTED FROM RGB IMAGES.



FIGURE 23 - OTHER DETAIL OF THE 3D MODEL

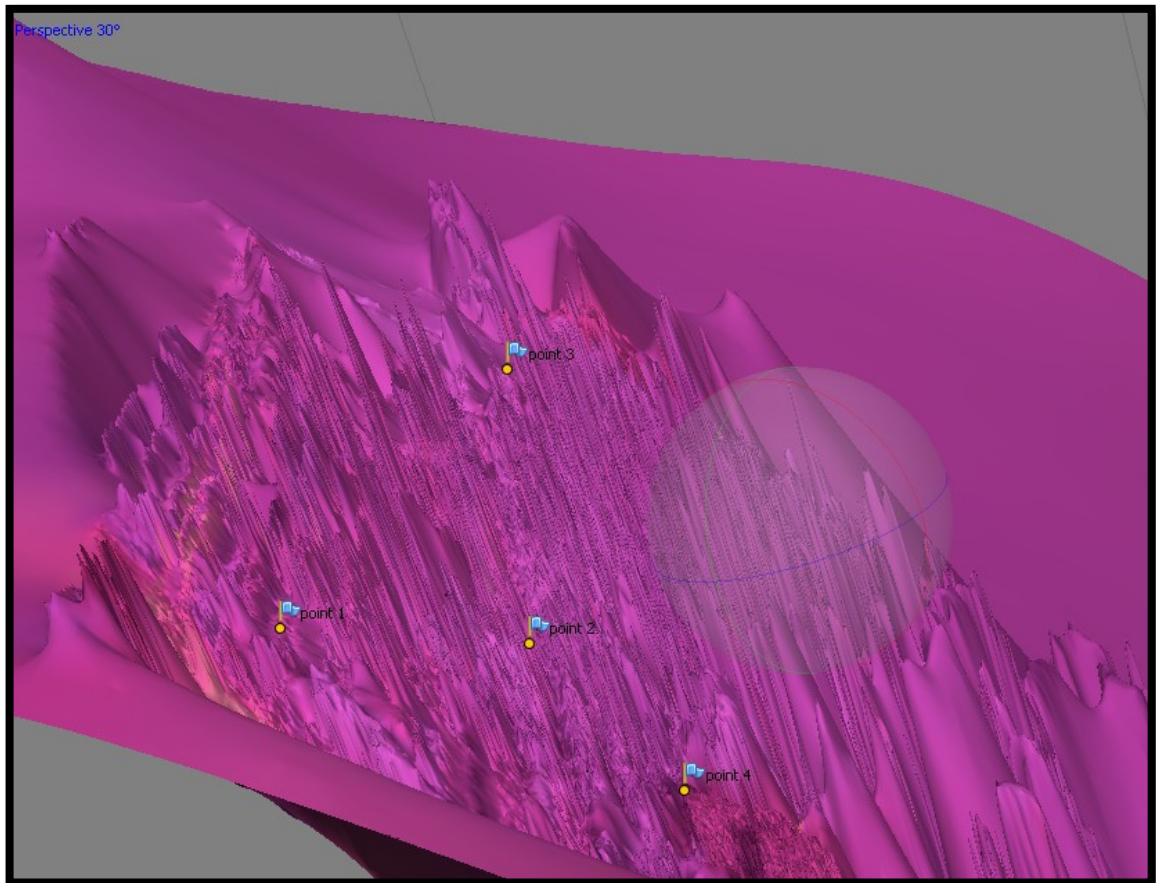


FIGURE 24 - 3D MODEL FROM RED-NIR BANDS IMAGES: IS POSSIBLE TO NOTICE THE HIGH LEVEL OF INNACURACY AND DISTORTION.

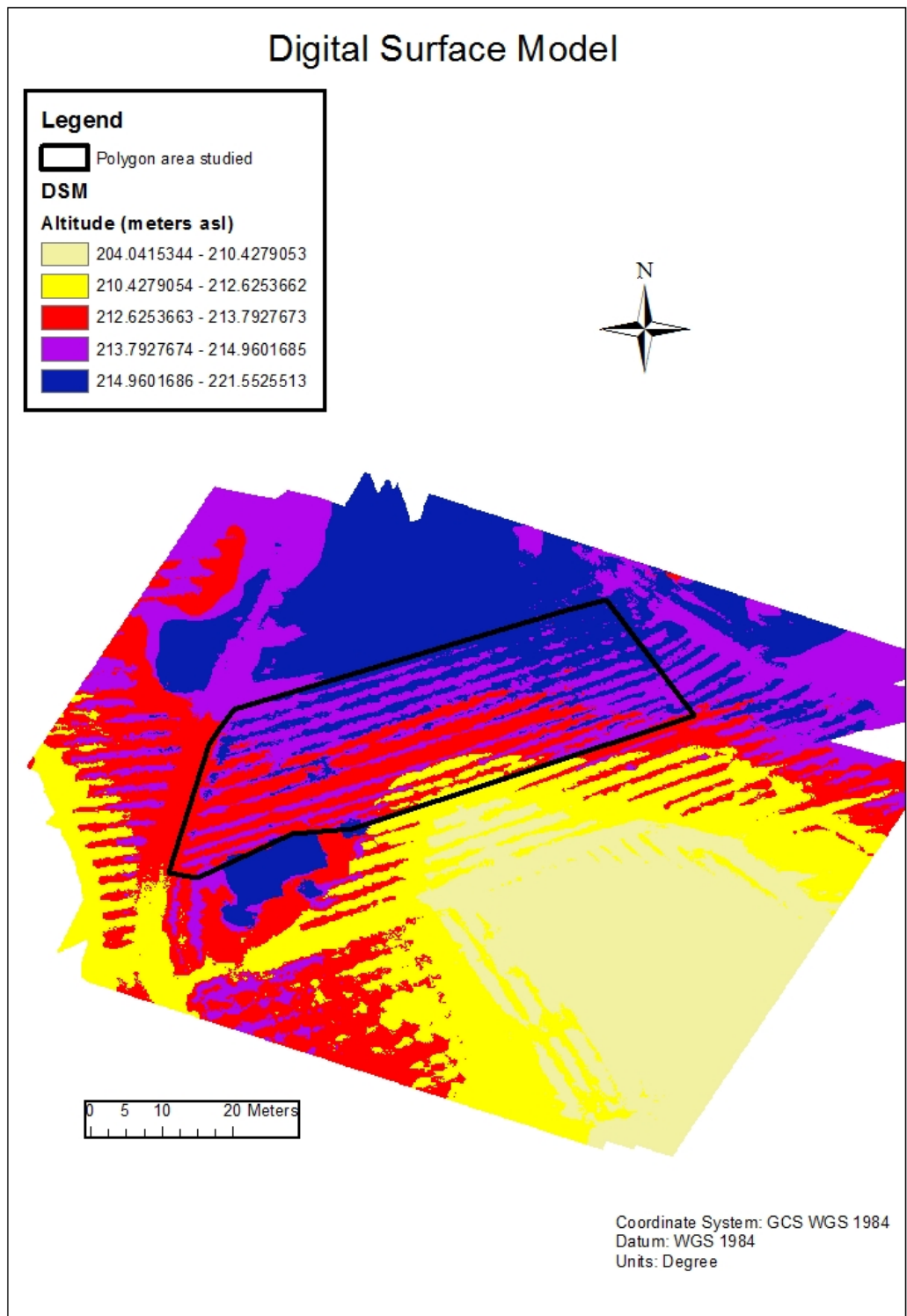


FIGURE 25 - MAP OF THE DIGITAL SURFACE MODEL IMPORTED IN ARCMAP.

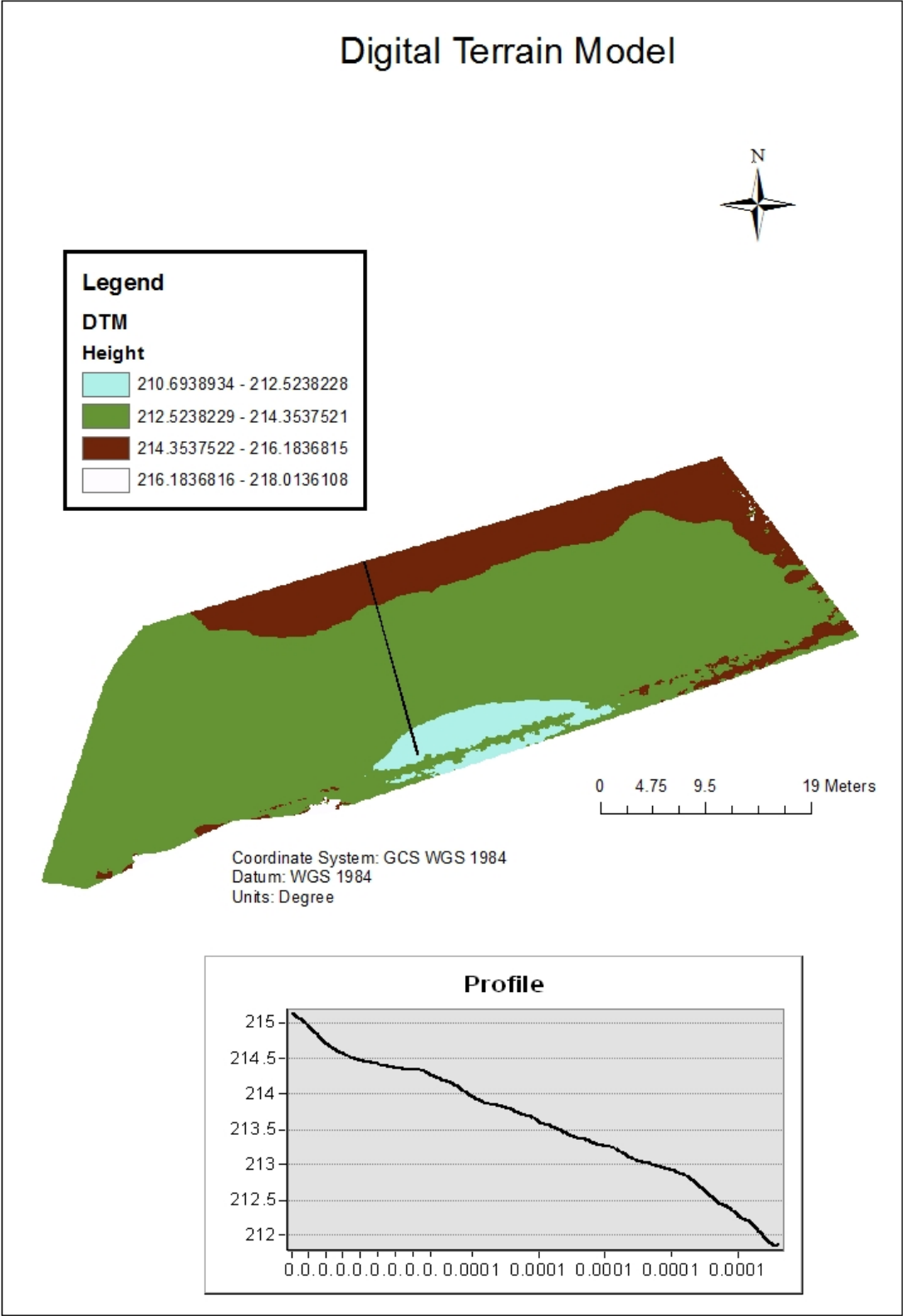






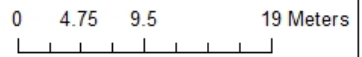
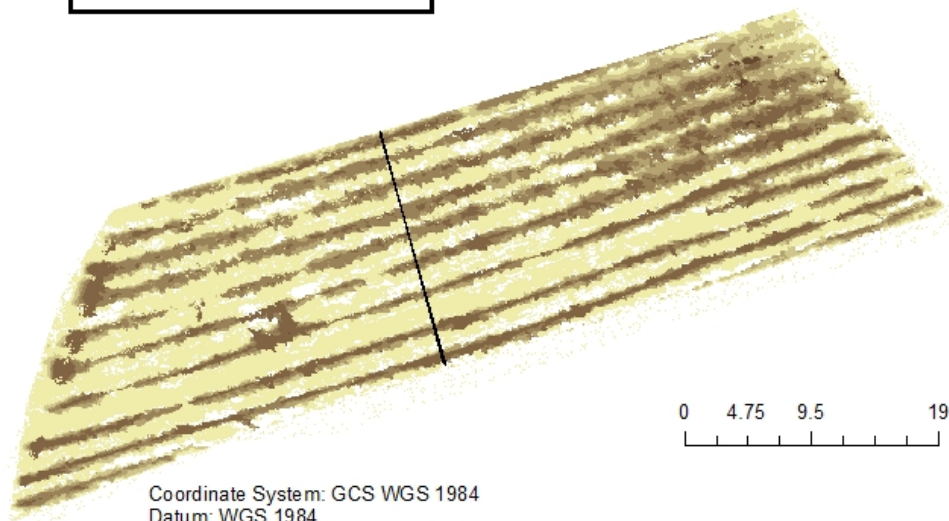


FIGURE 26 - MAP OF THE DIGITAL TERRAIN MODEL. IN THE GRAPH BELOW IS POSSIBLE TO OBSERVE THE PROFILE (HORIZONTAL DISTANCE IS EXPRESSED IN CHORDAL DISTANCE).

Digital Differential Model

Legend	
DDM	
Height	
	0.013634835 - 0.291625797
	0.291625797 - 0.746520099
	0.746520099 - 1.100326777
	1.100326778 - 1.403589645
	1.403589646 - 2.136474909
	2.13647491 - 3.40007019



Coordinate System: GCS WGS 1984
Datum: WGS 1984
Units: Degree

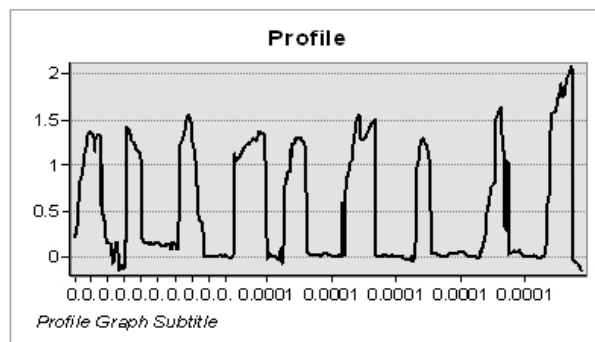


FIGURE 27 - MAP OF THE DIGITAL SURFACE MODEL. IN THE GRAPH BELOW IS POSSIBLE TO NOTICE THE PROFILE OF THE CANOPY (HORIZONTAL DISTANCE IS EXPRESSED IN CHORDAL DISTANCE).

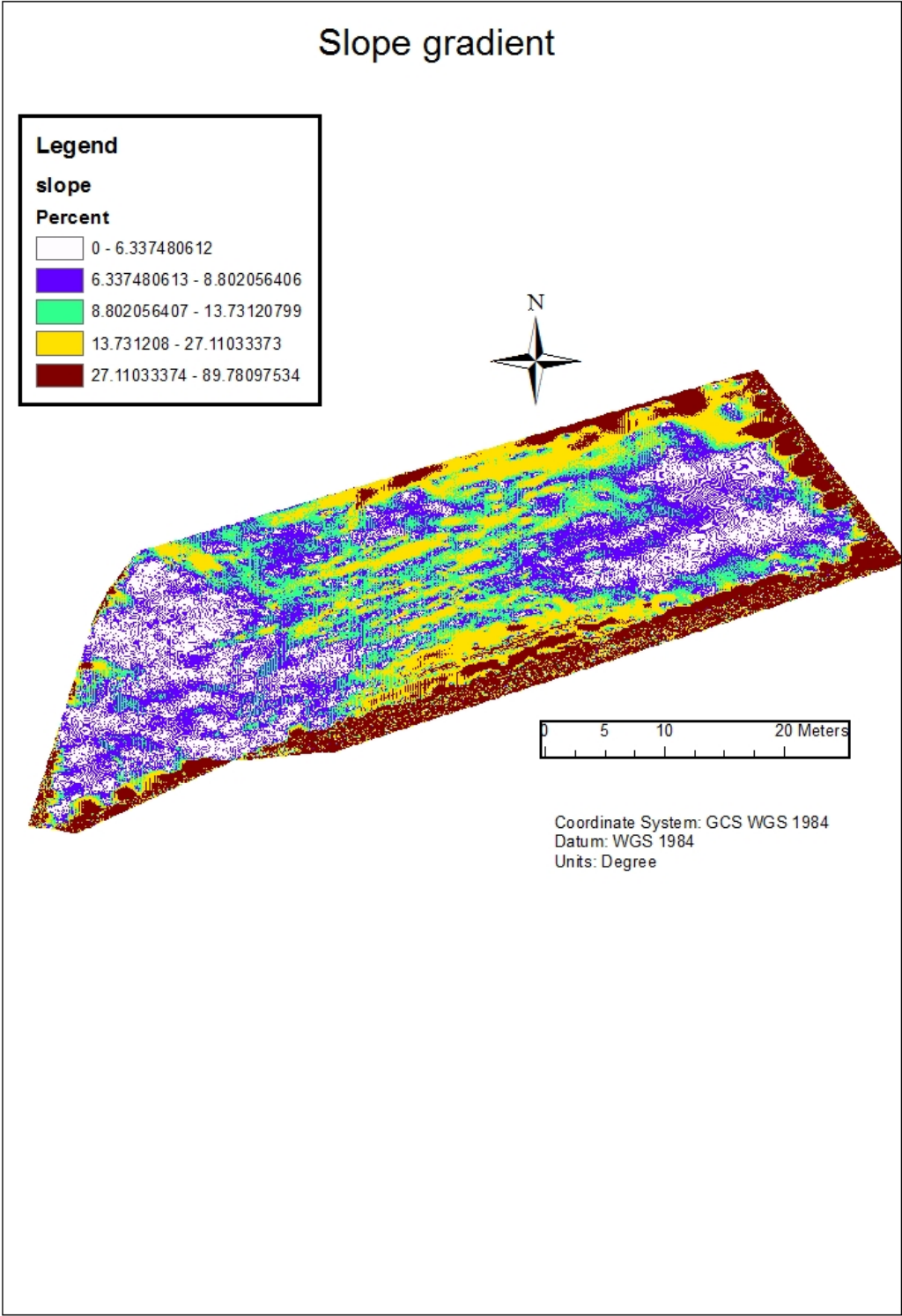


FIGURE 28 - MAP SHOWING THE SLOPE OF THE AREA STUDIED.

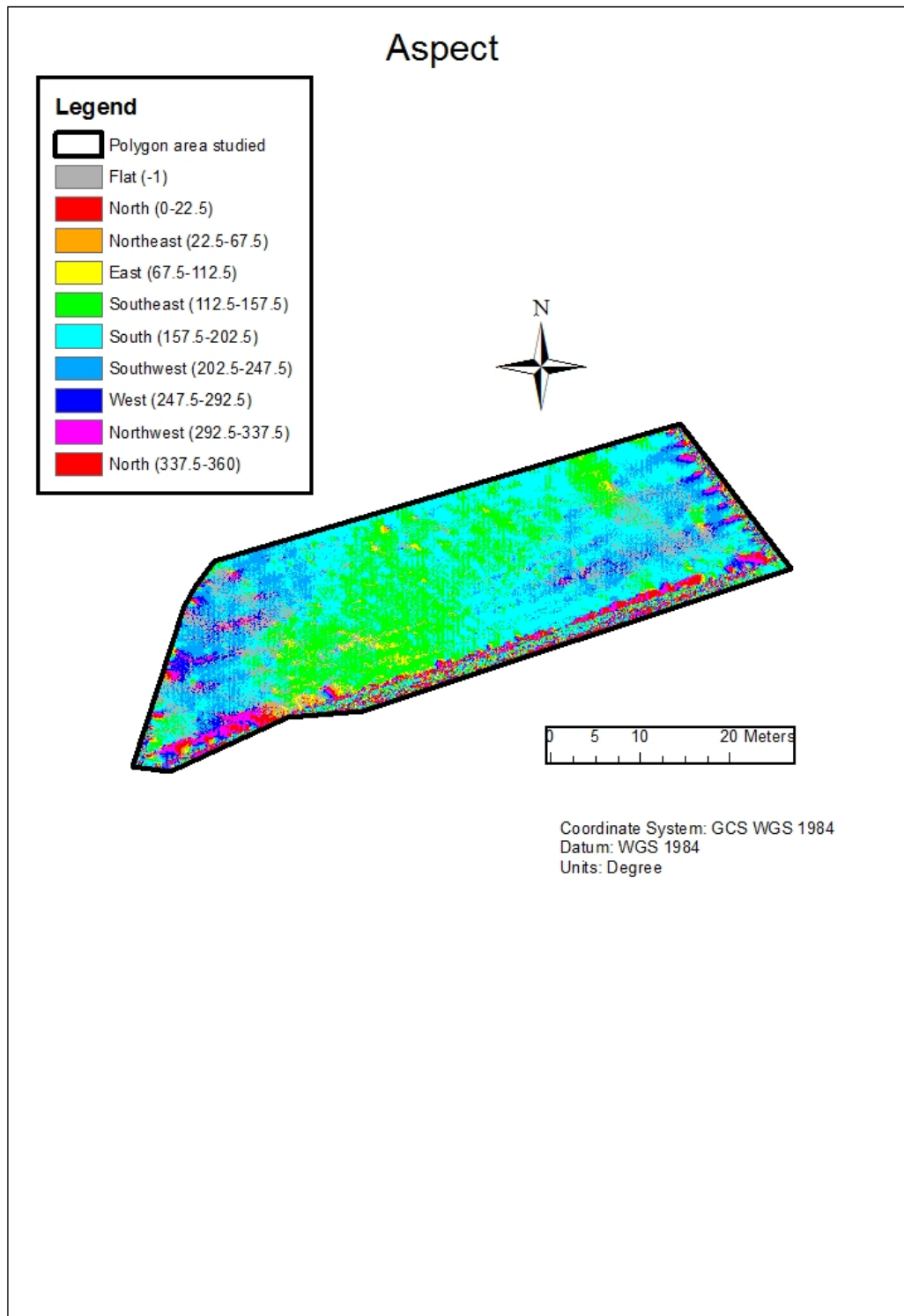


FIGURE 29 - MAP SHOWING THE ASPECT.



FIGURE 30 - ORTHOIMAGE OF THE AREA FROM RGB BAND IMAGES. IS POSSIBLE TO NOTICE SOME HOLES IN THE MODEL. THIS IS MORE EVIDENT IN THE IMAGE BELOW.

Orthoimage (red band)

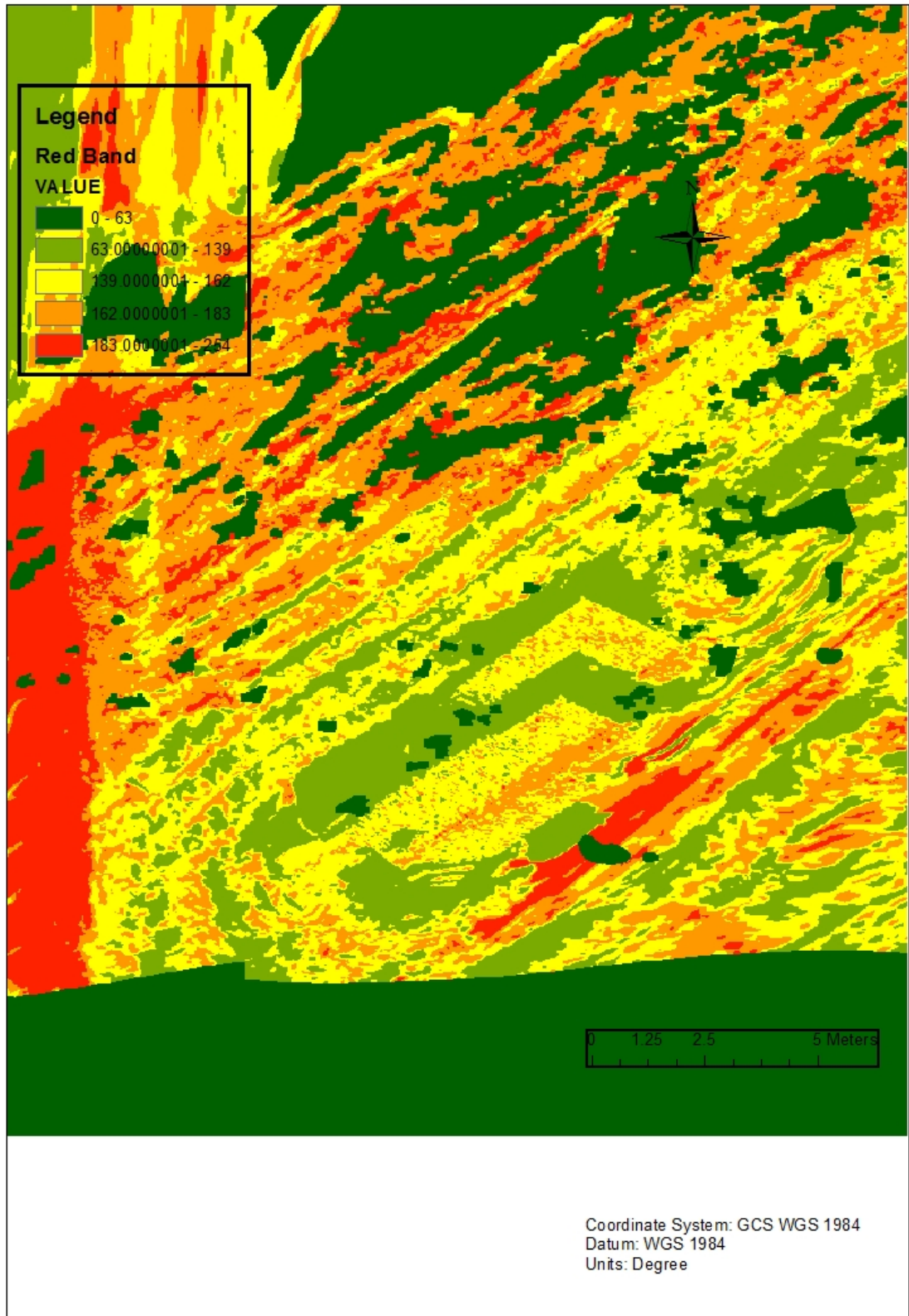


FIGURE 31 - ORTHOIMAGE IN THE RED BAND (FROM MAPIR CAMERA)

Orthoimage (Near Infrared Band)

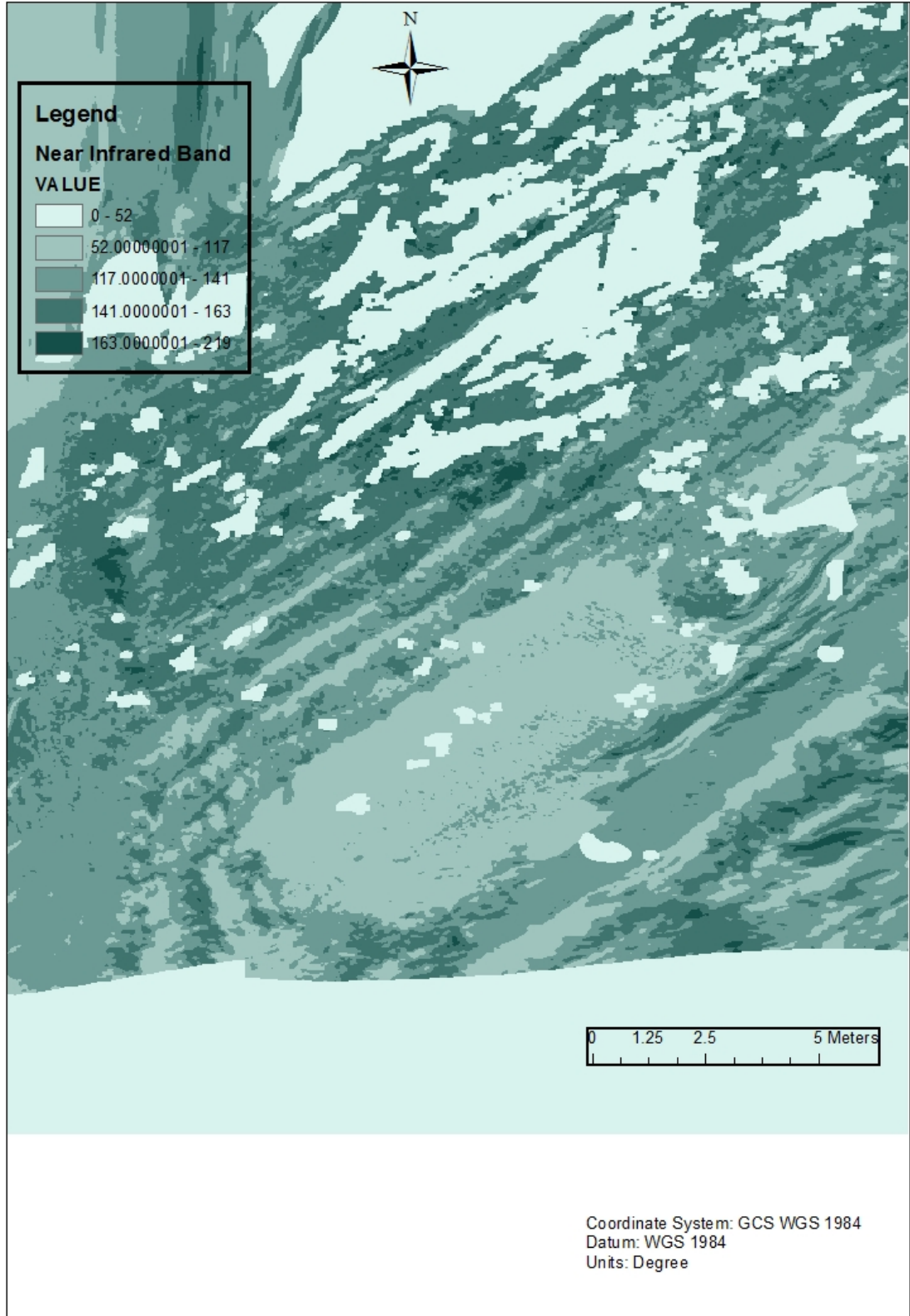


FIGURE 32 - ORTHOIMAGE IN THE NEAR INFRARED BAND (FROM MAPIR CAMERA).

Vineyard canopy after separation with eCognition

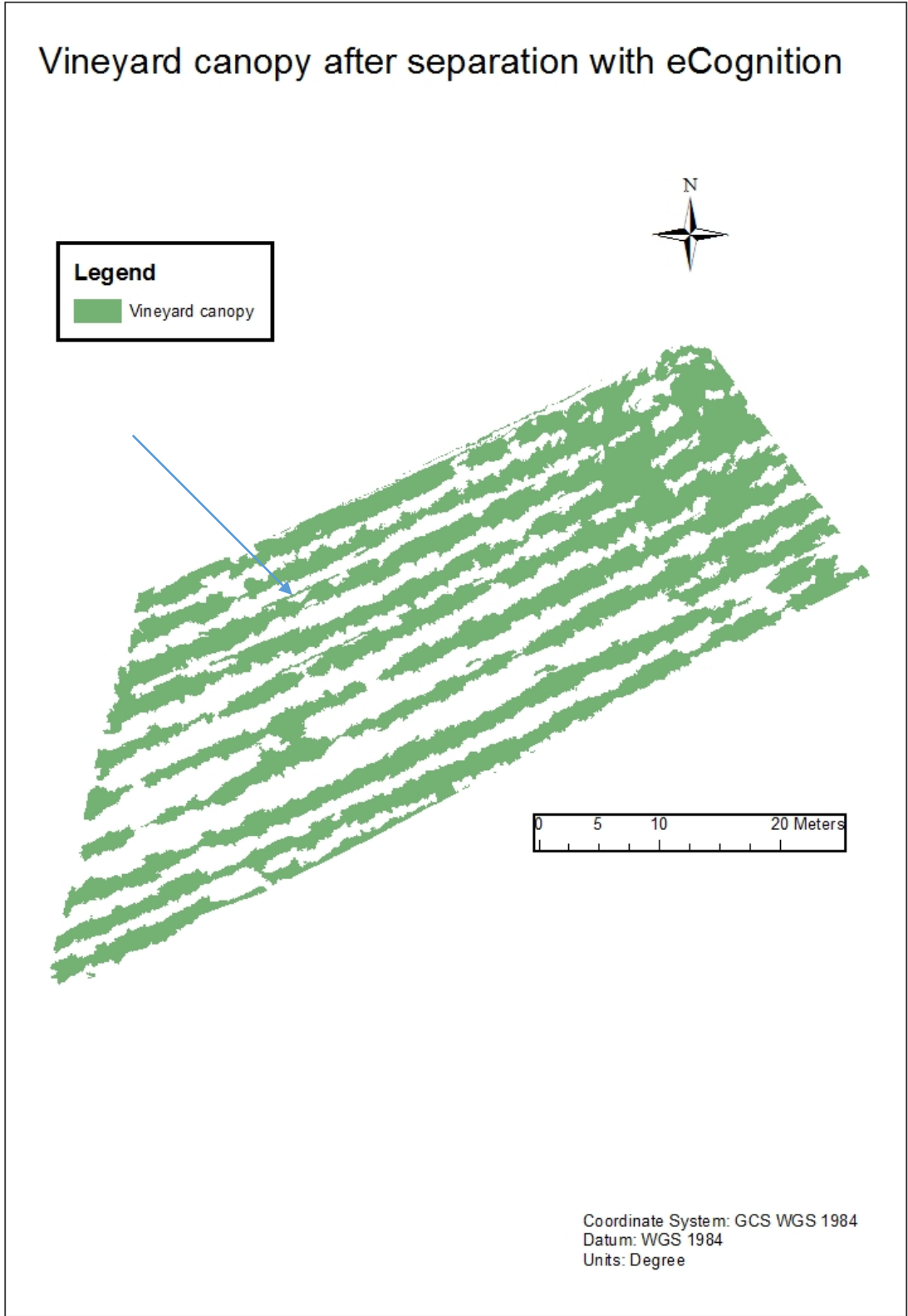


FIGURE 33 - RESULT OF CANOPY ISOLATION FROM ORTHOMOSAIC PERFORMED IN THE RGB BAND.

Topographic Wetness Index

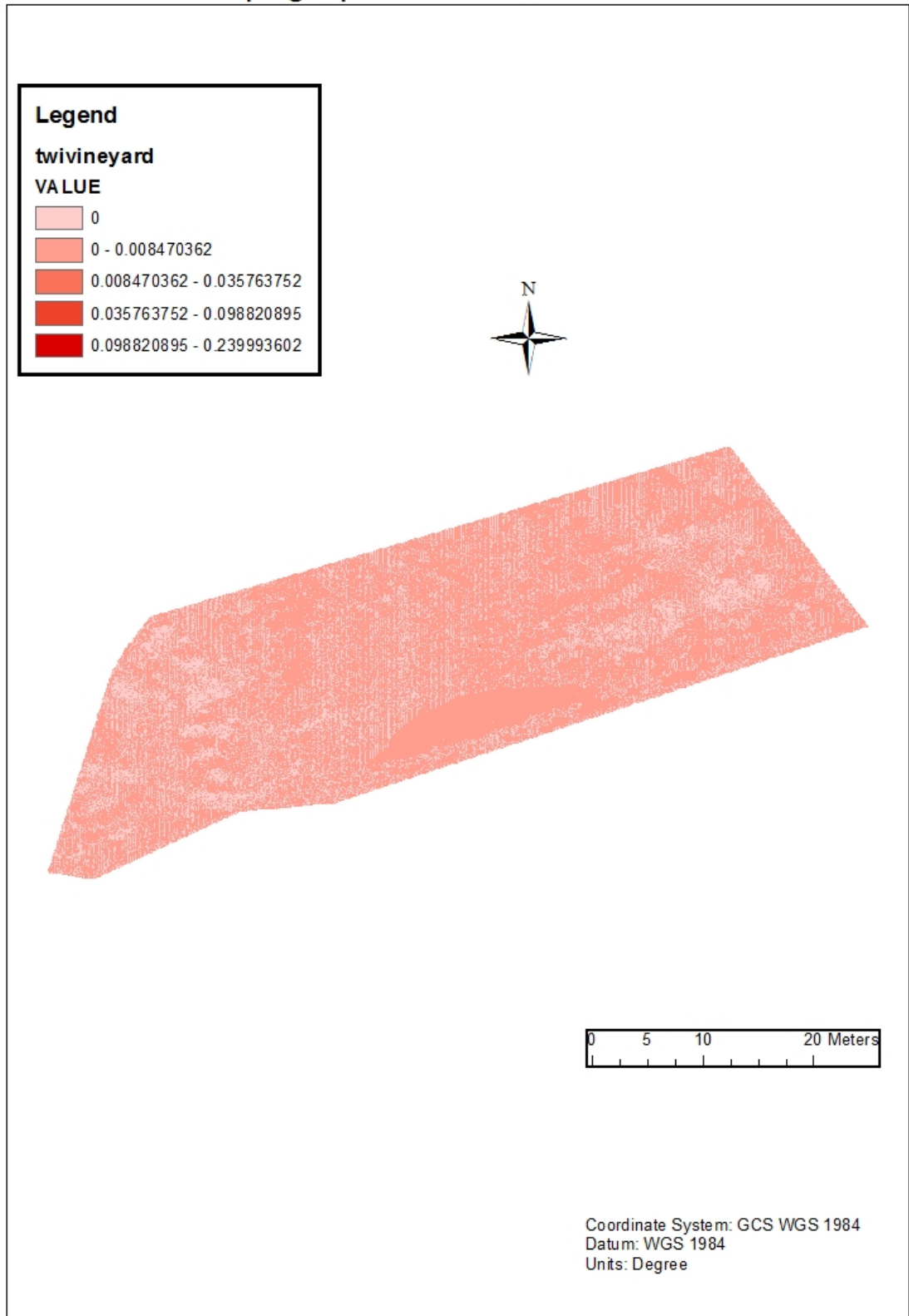


FIGURE 34 - MAP OF THE TOPOGRAPHIC WETNESS INDEX.

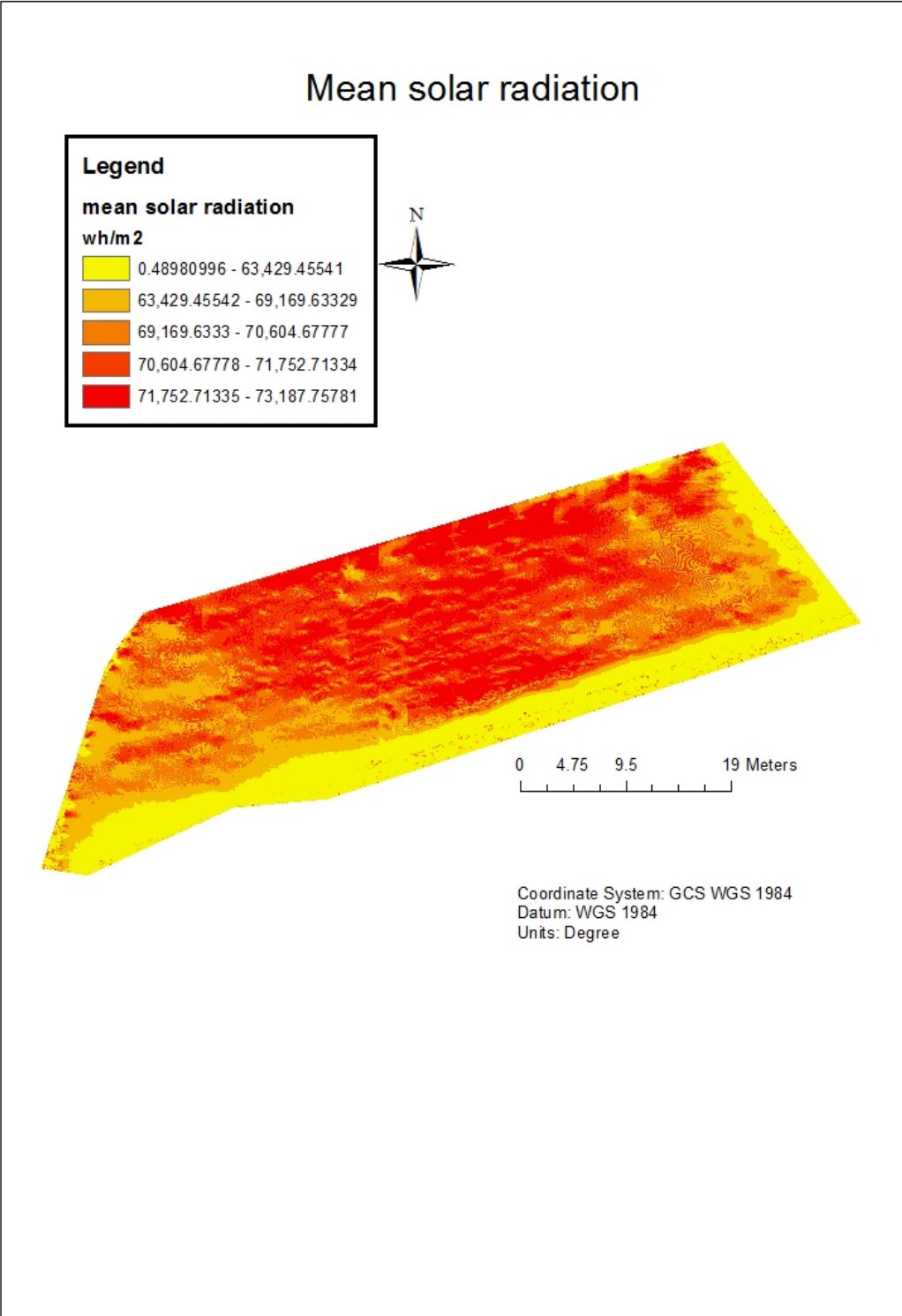


FIGURE 35 - SOLAR RADIATION: THIS MAP EXPRESSES THE AVERAGE FOR THE PERIOD APRIL-SEPTEMBER.

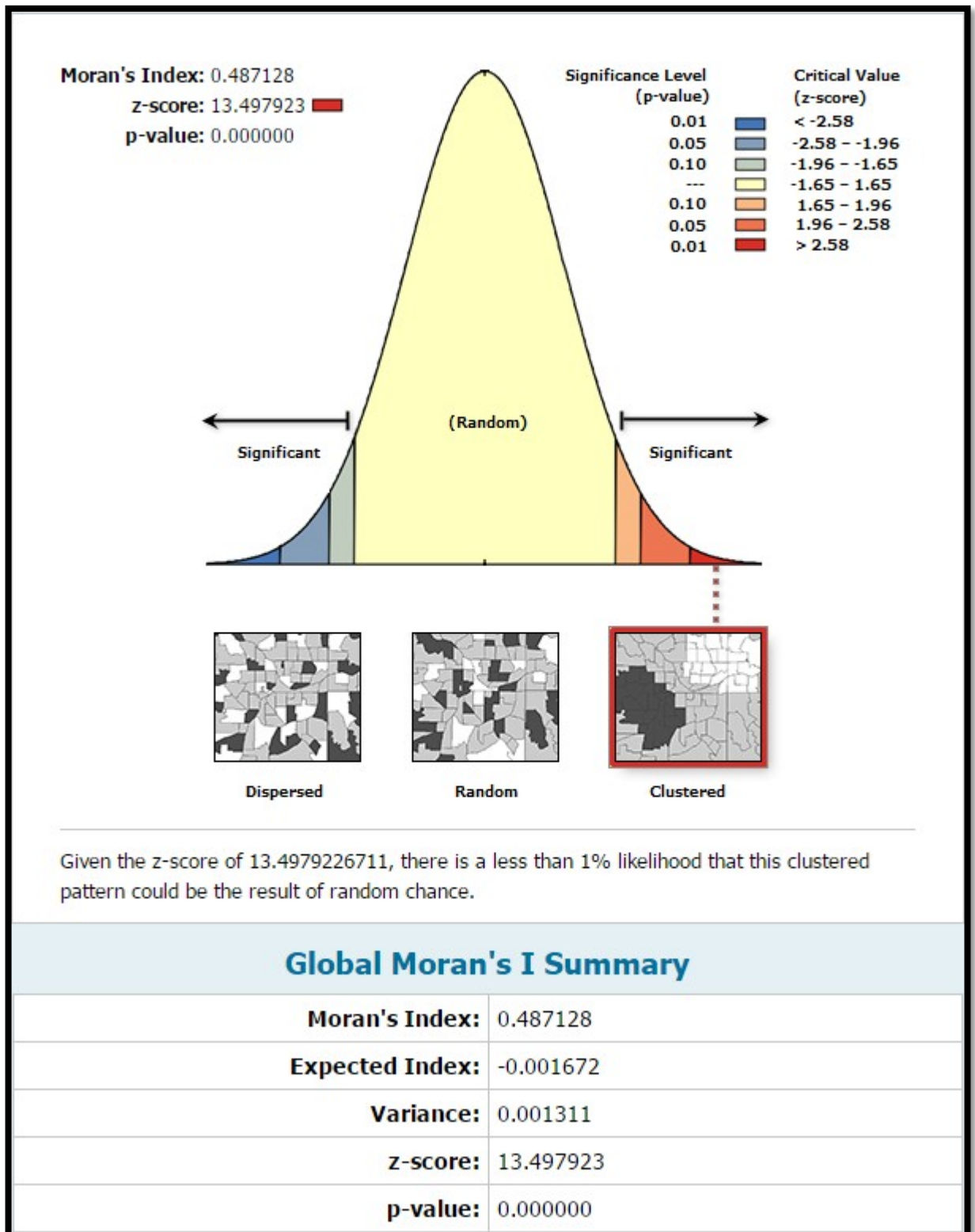


FIGURE 36 - SPATIAL AUTOCORRELATION FOR THE DIGITAL TERRAIN MODEL.

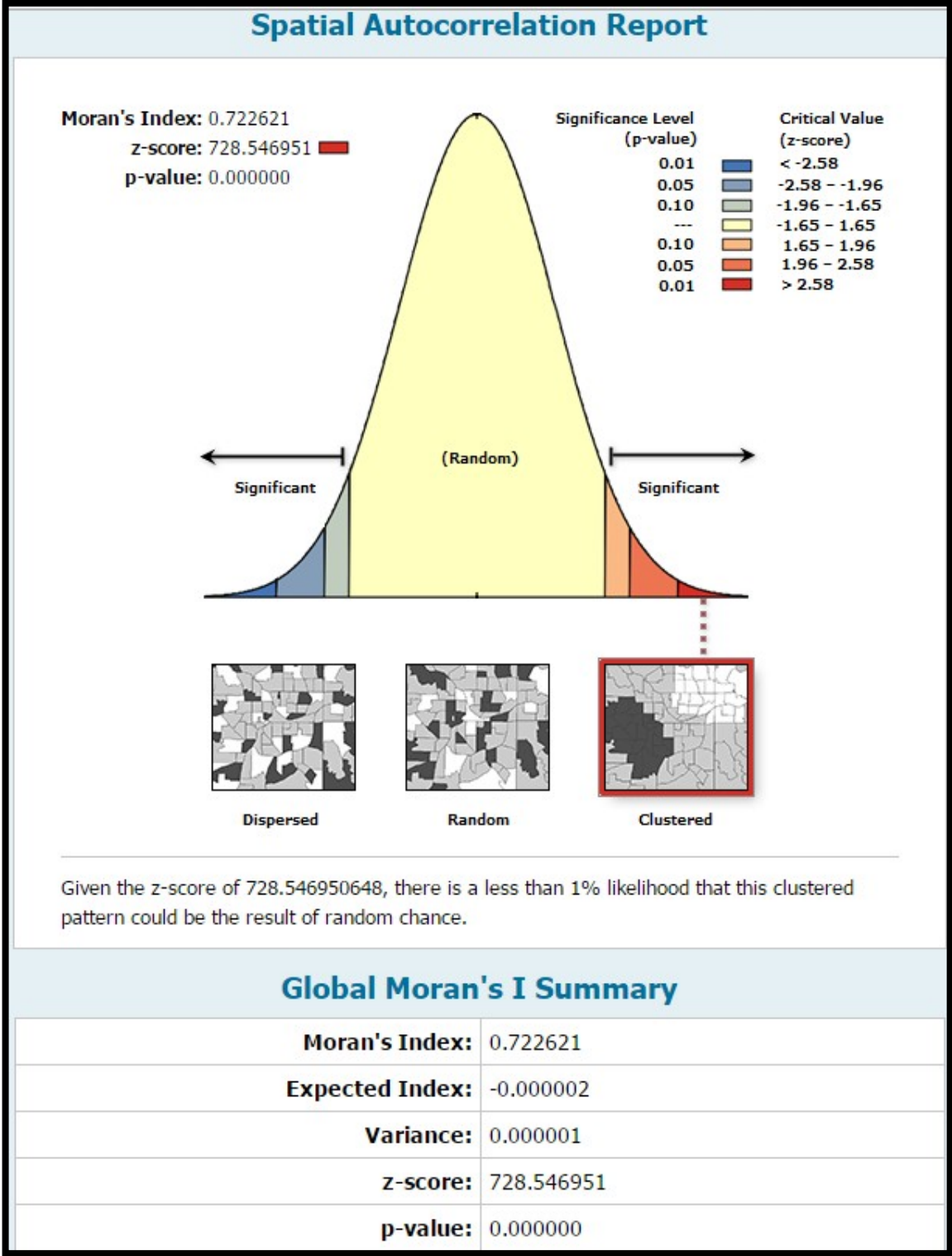


FIGURE 37 - SPATIAL AUTOCORRELATION FOR THE SLOPE FACTOR.

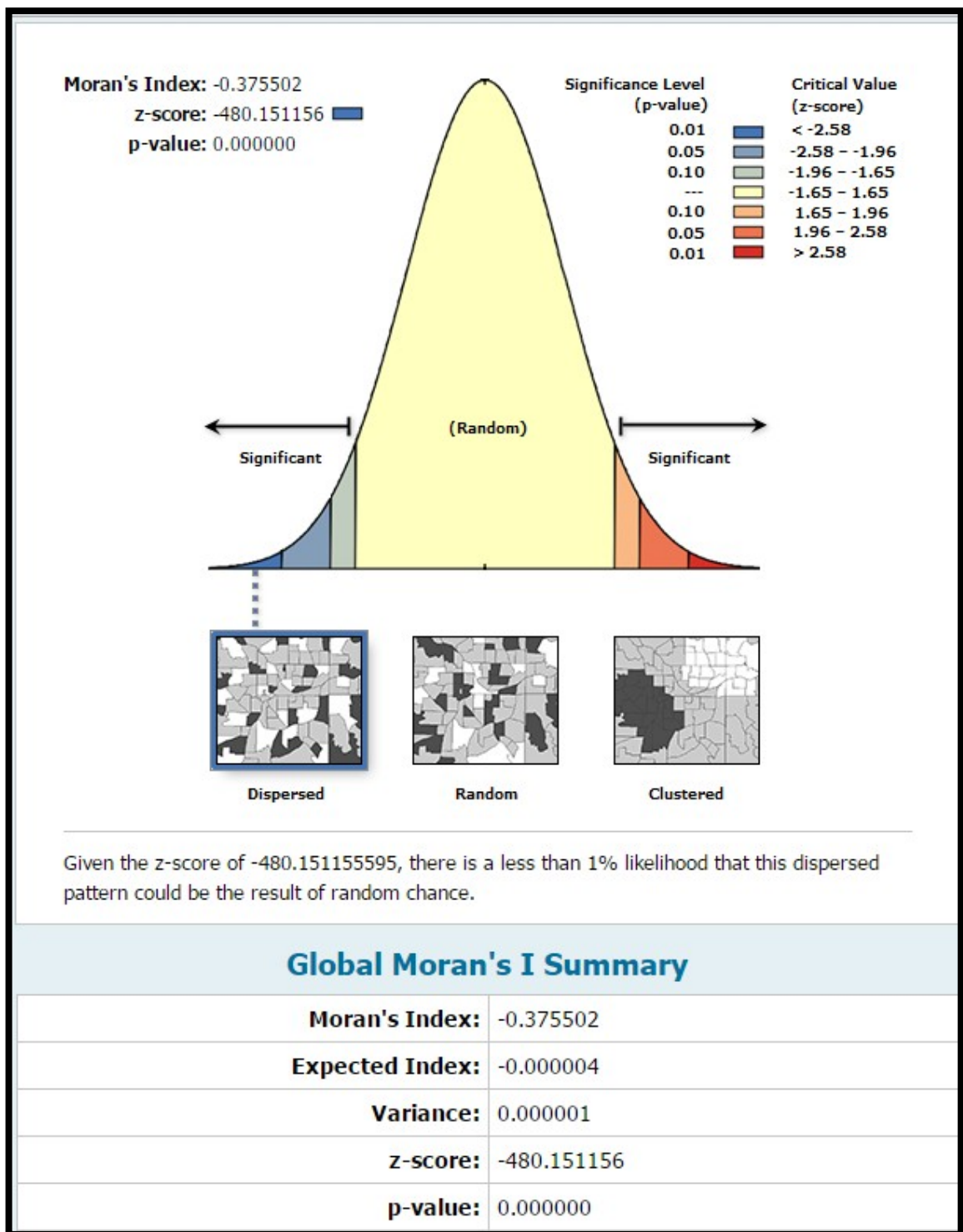


FIGURE 38 - SPATIAL AUTOCORRELATION FOR THE TOPOGRAPHIC WETNESS INDEX.

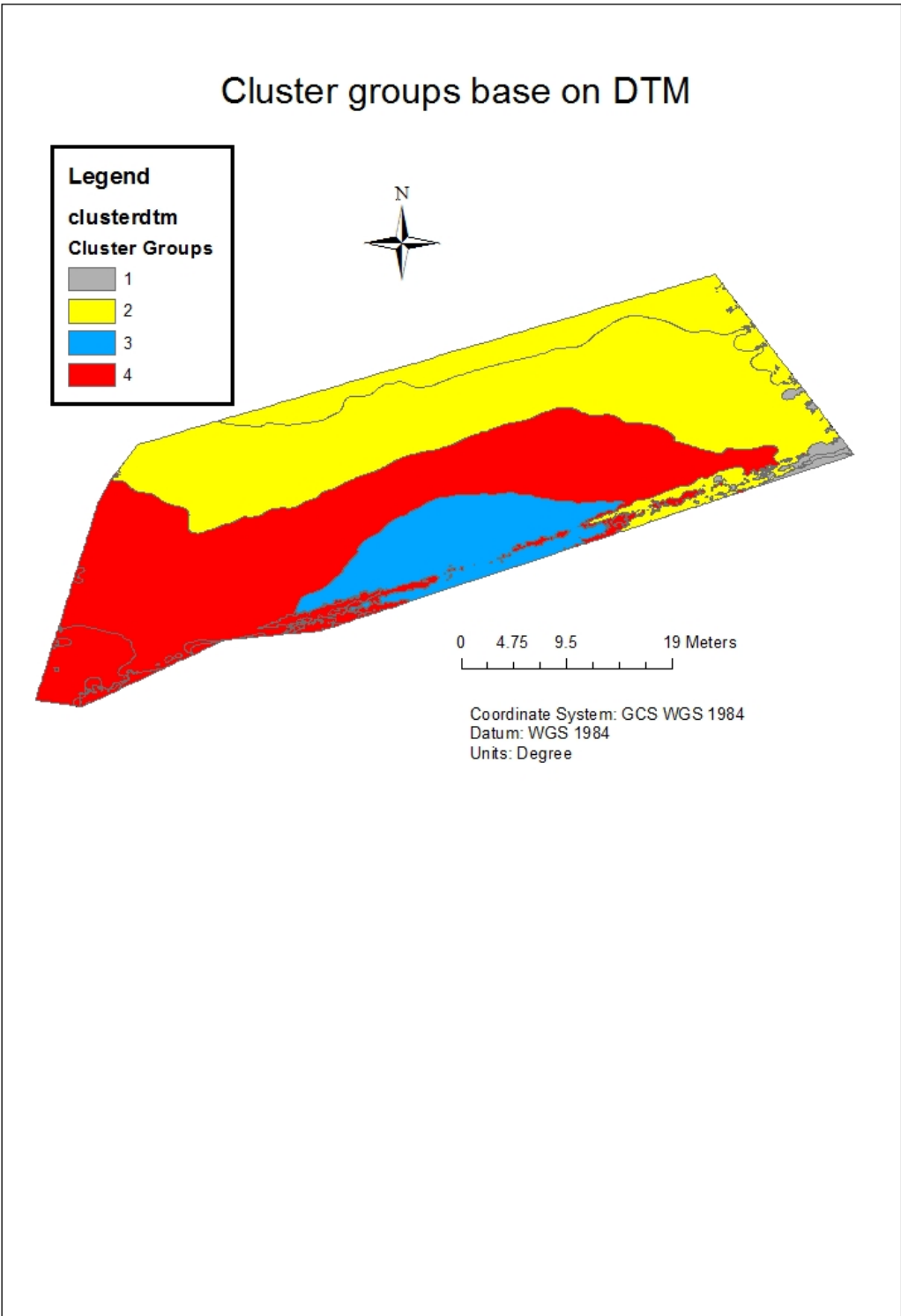


FIGURE 39 - CLUSTER GROUPS BASED ON DIGITAL TERRAIN MODEL.

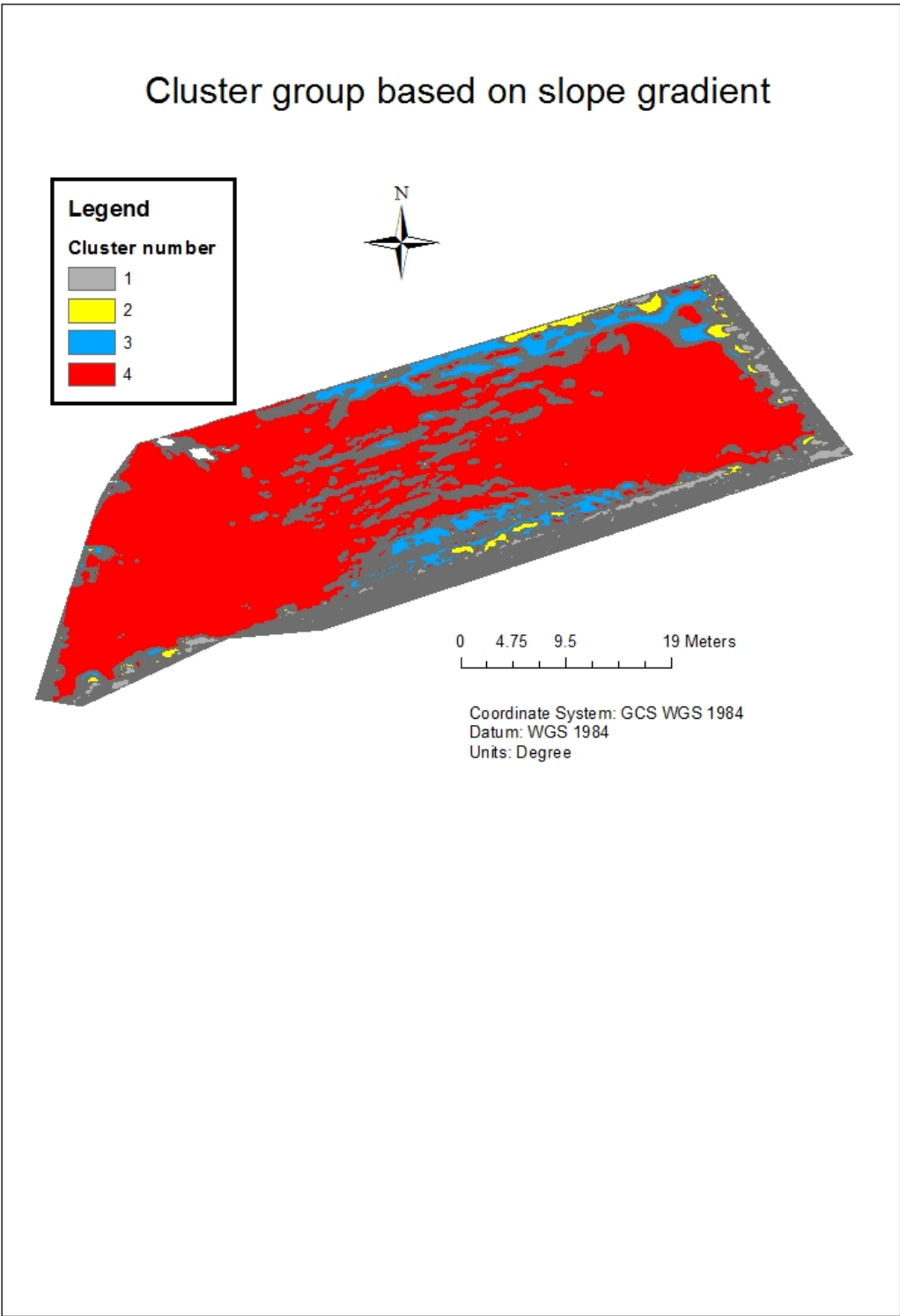


FIGURE 40 - CLUSTER GROUP BASED ON THE SLOPE GRADIENT

CHAPTER 5 – DISCUSSION

5.1 Introduction

The outcomes of the project are commented in this chapter and focus on UAVs and cameras evaluation, results obtained from photogrammetry and outcomes of cluster analysis.

5.2 Comment over the UAVS and cameras used

The aim of this project was to use affordable UAVs and camera sensors as a tool to gather data of the vineyards. In fact, the main idea of the project is that a person with basic experience should be able to collect images in a timely manner: is important to notice that a one-time data collection might offer erratic information and the temporal evaluation of mutable conditions could give more consistent results. One of the limiting factor which impeded the proper acquirement of Red-Nir images was the problem related with Tarot Gimbal: the shaking and instability impeded to capture still images at Nadir and thus a proper judgement over the Mapir camera cannot be performed.

Phantom 2 proved to be a very reliable platform and the learning curve to manoeuvre it is thus not very steep. In few hours an inexperienced operator could learn how to fly it and how to collect the data. The main limit on this drone is its inability to record flight coordinates and thence to have to information to geotag the images. However, the successive versions of Phantom have bypassed this problem and they have this capability. GoPro Hero 3+ Silver have proved to have an adequate resolution and an important fact to stress is that Agisoft Photoscan corrects properly the fish-eye distortion of the camera.

As mentioned formerly 3DR has some features which potentially could benefit inexperienced user: its main advantage is the possibility to program the flight path in a full automatic data collection and operator basically need to be able to set a user-friendly software on any Android tablet. Given the tiny size of the area studied the battery duration did not represent a limiting factor in this instance.

5.3 Canopy reconstruction

The canopy reconstruction with Agisoft Photoscan was accurate for the RGB images even though a larger number of images could have added more detail to the model. As is possible to evince from the figures a negative effect is given by the canopy shadowing, leading to less accuracy in the lower part of the plants. However, the model created with the Red-Nir images showed a high level of inaccuracy in conjunction with the presence of no-data in many parts of the model: this fact is mainly imputable to the poor quality of the source images linked with the problems of the gimbal. In spite of the superior number of images loaded on the model and the higher camera resolution, the result was a distorted model with many holes. An attempt to perform the same process in Pix4DMapper has given similar if not worse outcomes. Is important to notice that this fact is not imputable to software failure as Mapir camera website suggests to use Pix4D as a processing software. Given the cameras resolution, the flight altitude was probably too low and could have been increased to avoid blurry images.

The main problem faced with Photoscan was the incompatibility in importing its output files within ArcGis, in particular for projecting the points cloud and Orthoimage. To avoid this problem the choice made was to work with Geographic coordinates instead of projected ones, applying a Z-factor correction in ArcGis where necessary. Attempts to import the 3D model in ArcScene were also unsuccessful.

Comparison made between on-field observation of the canopy height and the profile of digital differential model showed that there might be underestimation of it.

The canopy isolation performed with eCognition using a basic algorithm gave satisfactory results. Notwithstanding, the explanation of the positive outcomes could be found on the fact that the dried mowed grass between the row, interrupting the continuum of “greenness”, allowed a simple classification merely based on colour and texture. Other studies (Burgos et al, 2015) outlines the difficulty in separating the canopy from the green lawn only using RGB images. In fact, the impossibility to include the near infrared band in the segmentation process limited the accuracy.

5.4 Cluster analysis

The cluster analysis revealed the presence of clusters on the DTM and slope but not on the TWI. Appreciable information about clusters should probably be made analysing the entire farm and using as a variable the 4 bands Orthoimage of the vineyards. One additional aspect to be scrutinised would be the temporal variability in particular for what regards the vigour map. A cluster analysis performed in this condition could give more information. The results of cluster analysis reveal that probably the size of the plot is too small to distinguish difference that could lead to clusters in the Topographic Wetness Index.

CHAPTER 6 – CONCLUSIONS

The importance of the knowledge of variability inside the vineyards is frequently underestimated by farmers even due to lack of affordable tools to quantify it. The information acquired in this research point out how UAVs and photogrammetry can be used successfully to recreate the 3D model of a vineyard, with competitive advantage in terms of cost compare with Lidar. In this research low-cost equipment were used in order to propose an affordable tool to gather data and prove that, with a limited budget is possible to enhance the knowledge of a complex environment like the vineyard.

However, as this research points out, the reliability of low cost equipment needs further scrutiny and one-time data collection is not sufficient to prove the reliability of the proposed UAVs and cameras.

Besides, one important factor to take into account resides in the accuracy of the image geolocation: an accurate reconstruction of the scene requires proper geolocation of images and in order to attain this goal the employment of RTK GPS measurement is mandatory. Even if images can be geo-located using the flight log stored in the UAV's autopilot, still accuracy seems not adequate and coordinate measurement of GCPs with a simple GPS does not give the necessary precision.

Future study could be addressed in evaluating UAV equipped with low cost RTK-GPS as Navspark, briefly introduced in the methodology chapter. A possible configuration could be a dual RTK GPS system, one mounted on the UAV and acting as a rover and one on the ground station working as a base. In this way it should be possible to eliminate the problem of placing ground control points.

Is important to notice that a single collection of images reflect the situation of the moment but more important would be the measurement of temporal variation in a complex and mutable environment as the vineyards.

Even if most of the characteristics measured in this study are unmodifiable and do not allow any improvement in the short period they are important for example in case of future replanting of the vineyard. Is enough to recall the solar map showed previously: in a future plantation using a laser levelling grader it could be possible to move soil in a way to change the topography of the plot studied. Soil excavation and movement could modify the DTM, the Slope and Aspect and aid to improve the energy intercepted by the plants canopy and in the end allow enhancement of biomass produced. This could affect enormously the quality of the final product.

Furthermore, cluster analysis could give more comprehensive results I f applied to 4-bands Orthoimage of the entire farm, instead of just a small plot as this research does.

CITED REFERENCES

BREÂDA N. (2003) *Ground-based measurements of leaf area index: a review of methods, instruments and current controversies* Journal of experimental botany, vol. 54, no. 392, pp. 2403±2417, November 2003

BURGOS, S., MOTA M.A, D. NOLL A, B. CANNELLE (2015) *Use of very high-resolution airborne images to analyse 3d canopy architecture of a vineyard*, The International Archives of the Photogrammetry, Remote Sensing and Spatial Information Sciences, Volume XL-3/W3, 2015 ISPRS Geospatial Week 2015, 28 Sep – 03 Oct 2015, La Grande Motte, France

CANDIAGO S., REMONDINO F., DE GIGLIO M., DUBBINI M. AND GATTELLI M. (2015) *Evaluating multispectral images and vegetation indices for precision farming applications from UAV images* Remote sensing 2015, 7, 4026-4047; doi:10.3390/rs70404026

CARAMÉS C.R., DIAGO M.P., MARTÍN M.P., LOBO A. AND TARDAGUILA J. (2015) *Using RPAS multi-spectral imagery to characterise vigour, leaf development, yield components and berry composition variability within a vineyard* Remote sensing. 2015, 7, 14458-14481; doi:10.3390/rs71114458

COSTANTINI E. , PELLEGRINI S., BUCELLI P., STORCHI P., VIGNOZZI N., BARBETTI R., CAMPAGNOLO S. (2009) *Relevance of the Lin's and Host hydrological models to predict grape yield and wine quality* Hydrology and earth system science 13, 1635–1648, 2009

DI BLASI S.A, BENEDETTELLI S.B, BERTAMINI M.C, BIONDI BARTOLINI A.A., BRANCADORO L.D, GENESIO L. (2010) *Nuove tecniche di indagine multiscala per la valutazione della qualità in vigneto* www.infowine.com – rivista internet di viticoltura ed enologia, 2010, n. 1/3

FAHRENTTRAPP J., HAFELE M., SCHUMACHER P., GOMEZ C., GREEN D., (2015) *Identifying physiological differences in highly fragmented vineyards using nir/rgb UAV photography* Giesco

FIORILLO E., CRISCI A., DE FILIPPIS T., DI GENNARO S.F., DI BLASI S., MATESE A., PRIMICERIO J., VACCARI F.P. AND GENESIO L. (2012) *Airborne high-resolution images for grape classification: changes in correlation between technological and late maturity in a Sangiovese vineyard in central Italy* Australian journal of grape and wine research 18, 80–90, 2012

GIL E., GALLART M., LLORENS J., LLOP J., BAYER T., CARVALHO C.
Spray adjustments based on LWA concept in vineyard. Relationship between canopy and coverage for different application settings. Aspects of Applied Biology **122**, 2014
International Advances in Pesticide Application.

GREEN D.R., SZYMANVSKY M. (2012) *Monitoring, mapping and modelling the vine and vineyard: collecting, characterising and analysing spatio-temporal data in a small* IXe Congrès International des Terroirs vitivinicoles 2012 / IXe International Terroirs Congress 2012

HALL A., LAMB D.W., HOLZAPFEL B.P., LOUIS J.P. (2011) *Within-season temporal variation in correlations between vineyard canopy and wine grape composition and yield* Precision Agriculture (2011) 12:103–117 doi 10.1007/s11119-010-9159-4

JOHNSON L.F., ROKZEN D.E., YOUKHANA S.K., NEMANI R.R., BOSCH D.F., (2003) *Mapping vineyard leaf area with multispectral satellite imagery* Computers and electronics in agriculture 38 (2003) 33-44

KALISPERAKISA I., STENTOUMISA CH., GRAMMATIKOPOULOS B L., KARANTZALOSC K. (2015) *Leaf area index estimation in vineyards from UAV hyperspectral data, 2d image mosaics and 3d canopy surface models* The international archives of the photogrammetry, remote sensing and spatial information sciences, volume xl-1/w4, 2015 international conference on unmanned aerial vehicles in geomatics, 30 Aug–02 Sep 2015, Toronto, Canada

KRIEGLER F.J., MALILA W.A., NALEPKA R.F. AND RICHARDSON W., 1969. *Preprocessing transformations and their effects on multispectral recognition*, in:

Proceedings of the Sixth International Symposium on Remote Sensing of Environment,
University of Michigan, Ann Arbor, MI, p. 97-131

LLORNS J.C., CASAMADA J.L., JIL E., ESCOLA A., 2011. *Ultrasonic and lidar sensors for electronic canopy characterization in vineyards: advances to improve pesticide application methods* Sensors · December 2011 DOI: 10.3390/s110202177 ·

Source: PubMed

MANCINI F., DUBBINI M., GATTELLI M., STECCHI F., FABBRI S.

AND GABBIANELLI G. (2013) *Using unmanned aerial vehicles (uav) for high-resolution reconstruction of topography: the structure from motion approach on coastal environments* Remote sensing 2013, 5, 6880-6898; doi:10.3390/rs5126880

MALTESE A., TOSCANO P., DI GENNARO SF., GENESIO L., VACCARI FP., PRIMICERIO J., BELLI C., ZALDEI A., BIANCONI R. AND GIOLI B. (2015) *Intercomparison of UAV, aircraft and satellite remote sensing platforms for precision viticulture* Remote sensing 2015, 7, 2971-2990; doi:10.3390/rs70302971

MATHEWS A.J., * AND JENSEN J.L.R. (2013) *Visualizing and quantifying vineyard canopy LAI using an unmanned aerial vehicle (UAV) collected high density structure from motion point cloud* Remote sensing. 2013, 5, 2164-2183; doi:10.3390/rs5052164

MAZZETTO F., CALCANTE A., MENA A., VERCESI A. (2010) *Integration of optical and analogue sensors for monitoring canopy health and vigour in precision viticulture* Precision agriculture (2010) 11:636–649 doi 10.1007/s11119-010-9186-1

PRIORI S., MARTINI E., HELMHOLTZ U.F.Z., ANDRENELLI M.C., MAGINI S., AGNELLI A.E., BUCELLI P., BIAGI M., PELLEGRINI S., COSTANTINI E.A.C. (2012) *Improving wine quality through harvest zoning and combined use of remote and soil proximal sensing* Soil science society of America 77:1338–1348
doi:10.2136/sssaj2012.0376

PROFFITT T., BRAMLEY R., LAMB D., WINTER., (2006) *Precision viticulture – A new era in vineyard management and wine production* • Cooperative Research Center for Viticulture

ROSSETTI M., GASPARINETTI P., LANDONIO S., BIASI W., MASCHIO T., PERATONER C., TEOT G., GENOVESE D., ZANCO E. (2011) *Ridurre i costi in vigneto e aumentare la qualità con una gestione di precisione* • L'informatore agrario 29/2011

SANTESTEBAN L. G., GUILLAUME S., ROYO J. B., TISSEYRE B. (2013) *Are precision agriculture tools and methods relevant at the whole-vineyard scale?* Precision agriculture (2013) 14:2–17 doi 10.1007/s11119-012-9268-3

SENTURK S., SERTEL E., KAYA E.(2013) *Vineyard mapping using Object Based analysis* DOI: 10.1109/Argo-Geoinformatics.2013.6621881

TORRES SANCHEZ J.,, PENA BARRAGAN J.M., ARQUERO O., (2015) *Characterising olive tree geometric feature using unmanned aerial vehicles images*

Conference paper Olivebioteq 2014 international conference for olive trees and olive products

TURNER D., LUCIEER A. AND WATSON C. (2012) *An automated technique for generating georectified mosaics from ultra-high resolution unmanned aerial vehicle (UAV) imagery, based on structure from motion (SfM) point clouds* Remote sensing 2012, 4, 1392-1410; doi:10.3390/rs4051392

TURNER D.A, LUCIEER A., WATSON C. *Development of an unmanned aerial vehicle (UAV) for hyper resolution vineyard mapping based on visible, multispectral, and thermal imagery*

WALLACE L., LUCIEER A., MALENOVSKÝ Z., TURNER D. AND VOP'ENKA P. (2016)

Assessment of forest structure using two UAV techniques: a comparison of airborne laser scanning and structure from motion (SfM) point clouds Forests 2016, 7, 62; doi:10.3390/f7030062

ZHANG C., KOVACS J.M. (2012) *The application of small unmanned aerial systems for precision agriculture: a review* Precision Agriculture (2012) 13:693–712 doi 10.1007/s11119-012-9274-5

Web pages:

<http://www.arpa.veneto.it/dati-ambientali/dati-ambientali#-strong-open-data--strong->

<http://desktop.arcgis.com/en/arcmap/10.3/tools/spatial-statistics-toolbox/cluster-and-outlier-analysis-anselin-local-moran-s.htm>

<http://desktop.arcgis.com/en/arcmap/10.3/tools/spatial-analyst-toolbox/h-how-zonal-statistics-works.htm>

<http://pro.arcgis.com/en/pro-app/tool-reference/spatial-statistics/grouping-analysis.htm>

<http://pro.arcgis.com/en/pro-app/tool-reference/spatial-analyst/sample-applications-for-solar-radiation-analysis.htm>

<http://desktop.arcgis.com/en/arcmap/latest/tools/spatial-analyst-toolbox/applying-a-z-factor.htm>

<http://desktop.arcgis.com/en/arcmap/10.3/tools/spatial-statistics-toolbox/how-grouping-analysis-works.htm>

<http://www.navspark.com.tw/high-precision/>

<http://blogs.reuters.com/counterparties/files/2013/10/Global-Wine-Shortage.pdf>

www.prosecco.it

<https://www.e-education.psu.edu/geog883/node/599>

<http://pro.arcgis.com/en/pro-app/tool-reference/spatial-statistics/grouping-analysis.htm>

<http://www.mapir.camera/pages/processing-survey2-images>

APPENDICE – CLIMATIC DATA

Temperature minimum in degree centigrades

Day	January	February	March	April	May	June
1	-1.3	2	5.9	10.5	9.4	12.2
2	-1.8	3.5	4.8	10.2	10.4	13.3
3	0.9	5.5	3.4	10.6	10.9	12.5
4	-1.5	0.7	2.1	9.3	10	14.8
5	-2.8	0.2	3.9	9.4	9.1	15.2
6	1.2	2.5	3.4	9.7	11.2	15.4
7	0.3	3.4	3.2	12.2	11.2	15.5
8	-0.4	5.6	2.7	10.7	11.6	15.4
9	4.2	5.7	3.5	9.7	13.3	15.1
10	3.8	3.4	5	10.4	13	14.3
11	5.7	1.3	6.5	10.3	12.1	15.7
12	4.2	2.1	6.3	8.6	10.4	14.1
13	2.4	0.6	6.3	10.7	9.9	14.3
14	0.7	2.5	5.3	10.7	12.3	14.6
15	0.8	3.6	2.6	10.6	9.3	14.7
16	-0.7	5.7	2.3	10.3	8.6	16.1
17	-3	4.4	5.1	11.4	7.7	15.3
18	-1.8	3.4	5.1	11.3	10.2	14.2
19	-4	4.2	6.1	10.4	10.9	14.8
20	-2.9	2.8	6.8	10.1	9.8	15.7
21	-3	1.7	5.5	8.8	13.4	15.5
22	-1.2	4	6.2	9.2	14.7	18.4
23	-0.6	7	5.5	11.3	10.9	20.9
24	-1.1	5.3	2.7	5.8	10.3	21.7
25	-0.1	3.8	5.3	4.4	11.5	18
26	0.9	3.1	4.5	5.5	14	18.7
27	0.7	4	5.7	4.9	15.5	17.7
28	1.9	5.8	8.3	4	16.2	15.9
29	3	6.7	7.4	5.6	13.6	17.8
30	4.4		9.5	7.5	13.7	19.3
31	4.6		10.9		12.7	
Minimum	-4	0.2	2.1	4	7.7	12.2
Average	0.4	3.6	5.2	9.1	11.5	15.9
Maximum	5.7	7	10.9	12.2	16.2	21.7
Average for the period	7.6	°C				

Temperature – Mean in degree centigrades

Day	January	February	March	April	May	June
1	1.9	6.1	8.9	13.6	11	15.8
2	0.6	5.7	8.1	14.9	14.1	15.6
3	2.8	6.6	4.9	15.3	16.1	16.9
4	1.1	5.9	7.1	11.2	17	17.5
5	2	5.5	5.6	15	14.7	18.2
6	3.4	6.2	6.2	15.5	17.1	19.7
7	2.6	5.2	4.9	16.4	17.5	20.8
8	3.7	7.2	4.3	14.7	17.4	18.8
9	5.2	7	6.3	11.4	16.2	17
10	5.8	6.6	9.6	14.6	15.5	19.5
11	7.3	5.6	9.6	15.4	13.3	18.2
12	6.8	4.3	10.2	15	14.3	17.4
13	5.3	3.5	10.2	15.2	13.5	19.1
14	3.2	4.4	9.3	13.7	14.7	17.1
15	4	7.2	5.3	14.8	13	18.8
16	3.3	8.1	6.5	15.7	12	19.7
17	3.1	5.2	9.2	14.4	14.2	20.3
18	1.9	8.4	10.4	15.7	14.5	19
19	-0.6	7	11.1	14.3	12.5	17.7
20	-0.3	6.7	11.1	14.2	18	18.8
21	1	6.7	10.6	14.6	19.1	21.2
22	1.4	7	11.2	14.4	20.5	24.7
23	1.7	9.2	9.9	13.2	14.8	26.6
24	2.5	8.4	9.3	9.7	15.3	27.7
25	3.5	6.3	8.9	8.9	17.9	26
26	4.7	5.3	9.8	8.7	19.8	23.9
27	5.3	5	8.8	10	20.9	22.1
28	5.1	7.3	10.7	9	21.2	21.9
29	6.6	8.7	12	12	17.2	23.3
30	6.4		12.8	13.7	15.3	24.2
31	6.4		13.1		14.8	
Minimum	-0.6	3.5	4.3	8.7	11	15.6
Average	3.5	6.4	8.9	13.5	15.9	20.2
Maximum	7.3	9.2	13.1	16.4	21.2	27.7
Average for the period	11.4	°C				

Temperature – Maximum in degree centigrades

Day	January	February	March	April	May	June
1	6.9	9.7	14.1	16.5	13.3	18.9
2	2.3	7.2	11.9	19.3	20.2	20.3
3	5.8	9.2	7.4	20.1	22.5	22
4	4.8	12.5	12.5	13.3	23.5	21.4
5	5	11.2	8.1	21.9	20.3	24.1
6	6.6	10.8	10.8	20.9	22.3	26.7
7	5.9	7	6.5	20.7	24.3	27.2
8	8.9	9	6.5	18.2	24.1	24.3
9	6.5	8.3	10.2	14.5	20.1	19.6
10	8.2	8.5	15.4	20.5	18.6	23.9
11	9.1	12.2	13	21.5	14.8	21.7
12	10.4	7.9	14.9	21.5	18.8	22.2
13	9.9	6.9	14.2	20	16.9	24.2
14	4.7	6.2	13.5	18.8	18.1	20.3
15	8.5	12.1	8.2	18.3	18.1	24.7
16	8.8	11.5	10.7	21.5	17	24.1
17	8.7	6.2	14.8	16.4	20	25.1
18	6.9	14.3	16.2	22.5	18.3	24.5
19	4	10.8	16.5	19.4	14.1	23.8
20	4	11.6	15.6	19.7	24.8	25.3
21	6.8	12.3	16	20.9	24.3	26.7
22	5.5	10.6	16	19.9	26.7	30.5
23	5.9	12.3	15.3	17.4	18.5	31.3
24	6.9	11.8	15.5	11.7	19.5	33.1
25	8	8.5	12.6	14.7	23.6	32.2
26	9.7	7.4	16	12.9	25.7	28.6
27	10.3	6.3	10.7	17.2	27.1	27.7
28	10.6	10.9	13.8	14.3	26.5	27.9
29	10.4	11.5	15.5	18.1	20.8	28.8
30	8.7		16.2	19.5	18.8	30
31	10.1		17.5		17.5	
Minimum	2.3	6.2	6.5	11.7	13.3	18.9
Average	7.4	9.8	13.1	18.4	20.6	25.4
Maximum	10.6	14.3	17.5	22.5	27.1	33.1
Average for the period	15.8	°C				

Rainfalls (mm)

Day	January	February	March	April	May	June
1			0.4		12.2	0.4
2	6.8	0.6	0.6		2.2	13.2
3	7.2	9.2	17.2			0.2
4				0.2	7.6	1.8
5	0.4		63		11.2	25.6
6			2			
7		52	4.2			0.2
8		31.4	6.4	21.8		19
9	13.4	31	2	22.6		1.4
10	2.6	9.6			0.6	10.8
11	18.8				26.2	43.6
12	0.2	6.2			36.2	4.8
13		0.2		11.2	0.2	0.8
14		11.8		3.6	10	2.6
15		10.4	2.2		17	6.8
16		5.2			2	1.6
17		31.2		1.8		0.4
18					1.4	
19		11.2		1.4	9.4	0.6
20						
21			5.2			>>
22						
23				10	18.4	
24				8.4	2	
25						16
26				1.6		10
27		12.2		0.4		1
28		52.8				
29		38			55.6	
30					13.4	
31					51	
Sum	49.4	313	103.2	83	276.6	160.8
Rainy days	5	14	8	9	16	14
Total for the period	986	mm				
Rainy days in the period	66	days				

Relative air humidity maximum (%)

Day	January	February	March	April	May	June
1	87	100	100	100	100	100
2	100	100	100	100	97	100
3	100	100	100	96	78	100
4	100	98	85	100	97	100
5	100	78	100	100	100	100
6	94	87	100	100	73	100
7	89	100	100	83	72	88
8	87	100	100	100	76	100
9	100	100	96	100	89	100
10	100	100	78	100	100	100
11	100	74	74	93	100	100
12	100	100	80	97	100	100
13	96	100	72	100	100	100
14	97	100	66	100	100	100
15	88	100	98	89	100	100
16	91	100	98	98	100	100
17	85	100	68	98	99	100
18	45	100	67	100	100	82
19	60	100	77	87	100	86
20	63	100	93	90	92	87
21	63	87	100	88	88	90
22	69	95	100	85	89	83
23	70	94	70	100	100	79
24	70	100	74	100	100	91
25	69	89	76	100	100	100
26	70	89	93	100	100	100
27	87	100	100	100	100	100
28	94	100	87	87	97	87
29	90	100	96	90	100	86
30	100		100	72	100	90
31	100		100		100	
Minimum	45	74	66	72	72	79
Average	86	96	89	95	95	95
Maximum	100	100	100	100	100	100
Average for the period	93	%				

Relative air humidity minimum (%)

Day	January	February	March	April	May	June
1	47	80	57	66	52	59
2	64	97	61	47	39	61
3	73	58	56	41	32	60
4	76	17	32	83	18	58
5	83	42	65	40	35	45
6	63	49	61	48	31	38
7	58	84	80	37	29	41
8	49	88	78	49	30	55
9	61	100	49	68	44	73
10	94	36	29	47	56	47
11	100	27	37	39	81	69
12	71	60	44	36	59	58
13	53	77	32	50	70	45
14	52	76	27	52	70	69
15	46	58	53	48	62	49
16	21	53	37	38	47	53
17	13	90	33	72	38	34
18	14	49	36	43	50	47
19	27	63	39	48	77	47
20	31	34	47	40	32	44
21	37	51	52	35	42	41
22	34	58	42	40	34	36
23	43	67	26	56	65	43
24	43	27	33	70	51	43
25	37	57	40	36	49	44
26	42	58	43	54	42	48
27	45	51	65	30	41	36
28	60	78	57	42	38	35
29	64	72	59	27	60	38
30	69		59	32	84	45
31	72		63		75	
Minimum	13	17	26	27	18	34
Average	53	61	48	47	49	49
Maximum	100	100	80	83	84	73
Average for the period	51	%				

Weather station data:

<i>Station</i>	<i>Valdobbiadene - Bigolino</i>
<i>Period</i>	<i>January 1, 2016 to June 30, 2016</i>
<i>Altitude</i>	<i>222 m</i>
<i>X coordinate</i>	<i>1733368 Gauss- Boaga molten</i>
<i>Y coordinate</i>	<i>5085364 West</i>

VALDOBBIADENE (TV)